

CONCRETE COLUMNS REINFORCED WITH ADVANCED COMPOSITE GRID STRUCTURES

A Thesis

Presented to the

Department of Civil and Environmental Engineering

Brigham Young University

Submitted as Partial Fulfillment

of the Requirements for the Degree

Master of Science

By

Jason Scott Earl

June 1998

This thesis, by Jason Scott Earl, is accepted in its present form by the Department of Civil and Environmental Engineering for Brigham Young University as satisfying the thesis requirements for the degree Master of Science.

David W. Jensen, Committee Chair

Steven E. Benzley, Committee Member

Fernando S. Fonseca, Committee Member

Date

T. Leslie Youd, Department Chairman

CONCRETE COLUMNS REINFORCED WITH ADVANCED COMPOSITE GRID STRUCTURES

Jason Scott Earl

Department of Civil and Environmental Engineering

M.S. Degree, June 1998

ABSTRACT

An experimental investigation has been conducted to determine the compressive characteristics of advanced fiber-reinforced polymer grids for concrete columns. The composite structures employ graphite circumferential rings and fiberglass longitudinal bars to form a three-dimensional composite structure. Three generations of advanced composite structures were constructed with varying geometry and strength of longitudinal and circumferential reinforcement. The influence of longitudinal bars and the spacing and strength of circumferential rings was investigated. The results demonstrate that the composite grid concept works. This study also provides insight into the relevant load transfer mechanisms, geometric issues, and dependence on material properties. The longitudinal bars modestly increase the axial stiffness, but have little effect on the strength. The circumferential rings significantly increase the axial compressive strength, without significantly affecting the axial stiffness. The results indicate that full containment would be the strongest configuration; however, thirty percent partial containment gives comparable strength and is more cost effective.

David W. Jensen, Committee Chair

Steven E. Benzley, Committee Member

Fernando Fonseca, Committee Member

Date

T. Leslie Youd, Department Chairman

ACKNOWLEDGMENTS

I would like to acknowledge all of those who have taken part in this research and been of help to me in my studies. A grant from the National Science Foundation has made much of this research possible as well as support from the United States Army Construction Engineering Labs (USACERL). Professor Steve Tsai and Julie Wang from Stanford University have included BYU in their research efforts and have lent their materials and expertise on many occasions.

Thanks and deep appreciation must also go to Dr. Jensen who has been instrumental in this research and a good portion of my structural engineering education. Also appreciated is the time and energy of Ryan Alder, Tamera Gaufin, Rodney Blake, Thomas Weaver and Mike Brown. The success of one is typically due to the help of many, and this work is no exception. However, my wife, Natalie must be given special credit as she has supported and encouraged me in this endeavor while pursuing her degree in Manufacturing Engineering and taking care of our baby boy. May she know of my love for her and all that she has sacrificed for our little family.

TABLE OF CONTENTS

1	INTRODUCTION	1
1.1	THE NEED FOR REHABILITATION OF CONCRETE STRUCTURES	3
1.2	CURRENT METHODS USED FOR REHABILITATION & SEISMIC RETROFIT	4
1.3	ADVANCED COMPOSITE REINFORCEMENT IN CONCRETE STRUCTURES	5
1.4	CONTAINMENT OF CONCRETE COLUMNS FOR SEISMIC CONSIDERATIONS.....	6
1.5	PARTIAL CONTAINMENT VS. FULL CONTAINMENT.....	7
1.6	PROJECT OBJECTIVE.....	8
2	EXPERIMENTAL APPROACH	9
2.1	DESCRIPTION OF 1 ST GENERATION COLUMNS	9
2.2	DESCRIPTION OF 2 ND GENERATION COLUMNS	11
2.3	DESCRIPTION OF 3 RD GENERATION COLUMNS	12
2.4	THE TEST MATRIX	12
3	COMPOSITE GRID MANUFACTURE.....	15
3.1	1 ST AND 2 ND GENERATION GRID MANUFACTURING.....	15
3.2	3 RD GENERATION GRID MANUFACTURING.....	16
3.3	STRAIN GAGE PLACEMENT	18
4	CONCRETE COLUMN MANUFACTURE.....	19
4.1	MIX DESIGN.....	19
4.2	PLACEMENT OF CONCRETE	20
4.3	CONTROL SPECIMENS	21
4.4	CURING.....	22
5	TEST FIXTURE SETUP	23
5.1	OVERVIEW OF TEST FIXTURE SETUP.....	23
5.2	DESIGN AND FABRICATION OF SULFUR ENDCAPS.....	24
5.3	DESIGN AND FABRICATION OF STEEL ENDCAPS.....	25
6	EXPERIMENTAL PROCEDURE.....	26
6.1	TEST SPECIMEN PREPARATION.....	26
6.2	DATA ACQUISITION	27
6.3	SPECIMEN TESTING	28

7	EXPERIMENTAL RESULTS.....	31
7.1	DATA REDUCTION PROCEDURE.....	31
7.2	FIRST GENERATION COLUMNS WITH 5.1 CM SPACING.....	31
7.3	FIRST GENERATION COLUMNS WITH 10.2 CM SPACING.....	34
7.4	SECOND GENERATION COLUMNS	36
7.5	COMPARISON OF FIRST AND SECOND GENERATION COLUMNS	38
7.6	THIRD GENERATION COLUMNS	40
8	FAILURE MODES.....	42
8.1	TYPICAL SHEAR FAILURE.....	42
8.2	1 ST GENERATION COLUMNS.....	43
8.3	2 ND GENERATION COLUMNS	48
8.4	3 RD GENERATION COLUMNS	50
9	DISCUSSION OF RESULTS	54
9.1	FAILURE MODES	54
9.2	STRESS-STRAIN BEHAVIOR	55
9.3	LOAD TRANSFER EFFECTS	55
9.4	OPTIMIZATION OF GEOMETRIC CONFIGURATION	56
9.5	PARTIAL VS. FULL CONTAINMENT	57
10	CONCLUSIONS AND RECOMMENDATIONS.....	63
10.1	CONCLUSIONS.....	63
10.2	FUTURE RESEARCH.....	64
10.3	RECOMMENDATIONS.....	66
11	REFERENCES	67

TABLE OF FIGURES

FIGURE 1 PHOTOGRAPH OF ADVANCED COMPOSITE GRID STRUCTURE.....	1
FIGURE 2 PHOTOGRAPH OF FIRST MODERN SUSPENSION BRIDGE DESIGNED BY TELFORD (1826).....	2
FIGURE 3 CORRODED CAP BEAM & COLUMN, HOOP & VERTICAL STEEL WEAKENED.....	3
FIGURE 4 INSTALLATION OF CARBON WRAPS USING ROBO-WRAPPER I™.....	4
FIGURE 5 COLUMN FAILURE CAUSED BY LACK OF TRANSVERSE REINFORCEMENT.....	7
FIGURE 6 1 ST GENERATION COLUMNS WITH 10 CIRCS, 5.1 CM (2.0 IN.) SPACING.....	10
FIGURE 7 1 ST GENERATION COLUMNS WITH 10 CIRCS, 10.2 CM (4.0 IN.) SPACING.....	10
FIGURE 8 2 ND GENERATION COLUMNS WITH 21 LONGIS, VARIED SPACING OF CIRCS.....	11
FIGURE 9 3 RD GENERATION COLUMNS, 18 LONGIS, 40, 80, & 100% CONTAINMENT.....	12
FIGURE 10 TEST MATRIX.....	13
FIGURE 11 PHOTOGRAPH OF END CIRCS FOR 1 ST AND 2 ND GENERATION COLUMNS.....	15
FIGURE 12 3 RD GENERATION COLUMN.....	15
FIGURE 13 PHOTOGRAPH OF PVC WITH 2 LAYERS OF FIBERGLASS.....	17
FIGURE 14 PHOTOGRAPH OF STRAIN GAGE PLACEMENT TEST.....	18
FIGURE 15 SONOTUBE® USED TO SPACE CIRCS.....	20
FIGURE 16 CONTROL SPECIMENS FOR 3 RD GENERATION COLUMNS – 6 INCH DIAMETER.....	21
FIGURE 17 3 RD GENERATION COLUMNS AFTER BEING POURED.....	22
FIGURE 18 5,000 KIP BALDWIN COMPRESSION MACHINE.....	23
FIGURE 19 1 ST GENERATION COLUMNS WITH SULFUR ENDCAPS.....	24
FIGURE 20 PULVERIZED SULFUR CAPPING INSIDE OF STEEL ENDPLATE.....	25
FIGURE 21 3 RD GENERATION COLUMN WITH STEEL ENDPLATES.....	25
FIGURE 22 1 ST AND 2 ND GENERATION COLUMNS PACKAGED FOR TRANSPORT.....	26
FIGURE 23 PHOTOGRAPH OF MEGADECK® DATA ACQUISITION SYSTEM.....	27
FIGURE 24 PLEXI-GLASS SHIELDS USED FOR PROTECTION DURING TESTING.....	28
FIGURE 25 PHOTOGRAPH OF CONTROL SPECIMEN.....	29
FIGURE 26 TYPICAL END FAILURE FOR 1 ST GENERATION COLUMN.....	29
FIGURE 27 CONTINUATION OF END FAILURE FOR 1 ST GENERATION.....	30
FIGURE 28 LOAD VS TIME FOR 1 ST GENERATION COLUMNS WITH 5.1 CM (2.0 IN.) SPACING.....	32
FIGURE 29 AXIAL STRESS VERSUS STRAIN FOR 5.1 CM SPACED 1 ST GENERATION.....	33
FIGURE 30 CIRCUMFERENTIAL STRESS VERSUS STRAIN FOR 5.1 CM SPACED 1 ST GENERATION.....	33
FIGURE 31 CIRCUMFERENTIAL STRESS VERSUS STRAIN FOR 10.2 CM SPACED 1 ST GENERATION.....	35
FIGURE 32 LONGITUDINAL STRESS VERSUS STRAIN FOR 10.2 CM SPACED 1 ST GENERATION.....	35
FIGURE 33 LOAD-TIME HISTORY SHOWING LOAD TRANSFER DUE TO CIRC FAILURE.....	36
FIGURE 34 AXIAL STRESS VERSUS CIRCUMFERENTIAL STRAIN FOR 2 ND GENERATION COLUMN.....	37

FIGURE 35	AXIAL COMPRESSIVE STRESS VERSUS STRAIN IN 2 ND GEN. LONGITUDINAL REINFORCEMENT	38
FIGURE 36	INFLUENCE OF LONGITUDINAL REINFORCEMENT ON 1 ST AND 2 ND GENERATION COLUMNS	39
FIGURE 37	INFLUENCE OF CIRCUMFERENTIAL REINFORCEMENT ON 1 ST AND 2 ND GENERATION COLUMNS ...	39
FIGURE 38	STRESS VERSUS STRAIN FOR 3 RD GENERATION WIOUTHOUT STEEL ENDCAPS	40
FIGURE 39	STRESS VERSUS STRAIN FOR 3 RD GENERATION WITH STEEL ENDCAPS	41
FIGURE 40	PHOTOGRAPH OF SHEAR FAILURE IN REINFORCED COLUMN	42
FIGURE 41	PRELIMINARY TEST AND END FAILURE FOR CONFIGURATION WITH 6 CIRCS, 5 LONGIS	43
FIGURE 42	PHOTOGRAPHS OF COLUMN A IN AXIAL COMPRESSION, SPALLING & END FAILURE	44
FIGURE 43	PHOTOGRAPHS OF COLUMN B IN AXIAL COMPRESSION, BROOMING OF THE LONGIS.....	44
FIGURE 44	PHOTOGRAPHS OF COLUMN C IN AXIAL COMPRESSION, FAILURE OF CIRC	45
FIGURE 45	PHOTOGRAPHS OF COLUMN O, END CIRC FAILURE BEFORE BUCKLING OF LONGIS	46
FIGURE 46	PHOTOGRAPHS OF COLUMN D IN AXIAL COMPRESSION, END FAILURE	46
FIGURE 47	PHOTOGRAPHS OF COLUMN D IN AXIAL COMPRESSION, DOUBLE CIRC FAILURE.....	47
FIGURE 48	PHOTOGRAPHS OF COLUMN E IN AXIAL COMPRESSION, END FAILURE	47
FIGURE 49	PHOTOGRAPHS OF COLUMN G IN AXIAL COMPRESSION, END FAILURE SHOWN	48
FIGURE 50	PHOTOGRAPHS OF COLUMN H IN AXIAL COMPRESSION, BROOMING OF LONGIS SHOWN	49
FIGURE 51	PHOTOGRAPHS OF COLUMN I IN AXIAL COMPRESSION, END FAILURE.....	49
FIGURE 52	PHOTOGRAPH OF COLUMN J IN AXIAL COMPRESSION, BUCKLING OF THE LONGS	50
FIGURE 53	COLUMN A IN AXIAL COMPRESSION, SHOWING RUPTURE & BUCKLING.....	51
FIGURE 54	COLUMN B IN AXIAL COMPRESSION, SHOWING FAILURE OF 4" END WRAPS.....	51
FIGURE 55	COLUMN C IN AXIAL COMPRESSION, FAILURE OF CONTAINMENT & RUPTURE OF CORE.....	52
FIGURE 56	PHOTOGRAPHS OF COLUMN D IN AXIAL COMPRESSION.....	53
FIGURE 57	COMPARISON OF 1 ST GENERATION COLUMNS BY AMOUNT OF CONTAINMENT.....	59
FIGURE 58	COMPARISON OF 2 ND GENERATION COLUMNS BY AMOUNT OF CONTAINMENT	60
FIGURE 59	COMPARISON OF 3 RD GENERATION COLUMNS BY AMOUNT OF CONTAINMENT	60
FIGURE 60	COMPARISON OF 2 ND AND 3 RD GENERATION COLUMNS BY AMOUNT OF CONTAINMENT	61
FIGURE 61	COMPARISON OF 1 ST , 2 ND , AND 3 RD GENERATION COLUMNS BY AMOUNT OF CONTAINMENT.....	62
FIGURE 62	PHOTOGRAPH OF FAN-SHAPED LONGI FOR 4 TH GENERATION COLUMNS	64
FIGURE 63	PHOTOGRAPH OF FAN-SHAPED LONGIS ON MANDREL	64
FIGURE 64	PHOTOGRAPHS OF 4 TH GENERATION COLUMN FILLED WITH HIGH STRENGTH CONCRETE.....	65

CHAPTER 1

INTRODUCTION

The term “composite” can mean many different things, particularly in structural engineering. As a method of construction, it is often thought synonymous with the combined use of steel and concrete to exploit the characteristics of those materials. In a more general sense; however, it can apply to any use of two or more dissimilar materials to produce effective and economical structures. This research encompasses a two year study on the “proof of concept” for using advanced composite material in concrete structures and this thesis focuses on a new methodology of reinforcing concrete columns with fiber-reinforced polymer grids. These advanced composite grid structures are composed of members that are placed circumferentially as well as longitudinally (see Figure 1). This method of reinforcement allows concrete columns to be subjected to greater loads before induced shear failure occurs due to axial compression.



FIGURE 1 PHOTOGRAPH OF ADVANCED COMPOSITE GRID STRUCTURE

Once this concept is proven effective through testing, a validated design criteria can be established which will allow composite reinforcement in concrete structures. These new materials will improve resistance to environmental deterioration, enhance ductility, and increase desirable damping characteristics [Dutta, 1998]. A validated design criteria also has the potential to revolutionize structural rehabilitation of existing concrete columns through enhanced seismic performance, reduced cost for infrastructure repair and increased longevity. In the future, “functional considerations” will lead to the choice of different materials for different parts of a structure [Braestrup, 1998]. These considerations will also allow for combinations of materials that exploit their individual qualities to produce advantages that are greater than the sum of the parts. Although the use of composites in modern infrastructure is still considered a new and relatively unknown field, this paradigm shift will not be the first one in engineering history. Almost 150 years ago, during the Industrial Revolution in Great Britain, a few engineers managed to break out of the conventions of their times to design with entirely new materials which changed the world forever. An example of this is the first modern suspension bridge designed and constructed by Thomas Telford in Great Britain (see Figure 2). This innovative design incorporated steel cables consisting of many hundreds of small diameter near-parallel wires totaling nearly 13,000 miles in length. Just as steel and concrete allowed for a radical change in the design of structures in the last two centuries, advanced composites will allow for structural innovations in the future.



FIGURE 2 PHOTOGRAPH OF FIRST MODERN SUSPENSION BRIDGE DESIGNED BY TELFORD (1826)

1.1 THE NEED FOR REHABILITATION OF CONCRETE STRUCTURES

Rapidly deteriorating infrastructure is reaching crisis proportions. Recent articles have iterated the problems of a decaying infrastructure, with nearly one quarter million bridges in the United States alone being structurally deficient [Dunker and Rabbat, 1995]. Although some of these deficiencies are due to ever-increasing traffic loads, a major cause is deterioration introduced by corrosion of reinforcing steel in concrete structures. Corrosion in reinforced concrete structures poses multiple problems. A porous material, concrete allows some fluids to penetrate. Water and alkalis penetrate the concrete and attack the steel reinforcement. Corrosion of the steel reinforcement causes the steel to expand. The forces caused by the expansion of the steel are enough to overcome the small tensile capacity of the concrete and cause the concrete to crack and spall. With failure of the concrete, the load transfer between the concrete and steel is lost and the reinforcement becomes useless (see Figure 3).



FIGURE 3 CORRODED CAP BEAM & COLUMN, HOOP & VERTICAL STEEL WEAKENED

Because of the prohibitive cost of replacing large numbers of decaying structures, efforts have focused on methods of strengthening existing structures [Saadatmanesh, et al., 1997]. The terminology for strengthening these existing structures varies somewhat; however, most structural engineers agree that rehabilitation refers to repair and upgrade of an earthquake-damaged structure to capacity larger than original while retrofit suggests improvement of load capacity

before the earthquake strikes. The seismic retrofit and rehabilitation of these concrete structures represents one of the most challenging problems faced by structural engineers today.

1.2 CURRENT METHODS USED FOR REHABILITATION & SEISMIC RETROFIT

Until recently, steel jacking was the only retrofitting method approved by the California Transportation Department. Steel jacking has been effective in preventing columns from collapsing due to shear or flexural failure [Saadatmanesh, et al., 1996]. Installation of steel jackets, however, is labor intensive and requires heavy equipment to handle the massive steel. A typical 1.2 m (4 ft.) diameter by 6.7 m (22 ft.) high circular column requires five 8-hour shifts, excluding site excavation and painting [Cercione and Korff, 1997]. Steel jackets also present another challenge. Jacket thickness and weight are determined by installation requirements rather than confinement requirements. For example, each jacket must be much heavier than otherwise required in order to prevent it from buckling under its own weight during lifting, placing and grouting. In most retrofit projects this method is both expensive and inefficient. An alternative to steel jackets is carbon-composite retrofit wrapping (see Figure 4), such as is being applied by the Xxsys Technologies Robo-Wrapper[®] [Gerfely, et al., 1997].



FIGURE 4 INSTALLATION OF CARBON WRAPS USING ROBO-WRAPPER ITM

Carbon fiber exhibits extraordinarily high strength and orthotropic stiffness. A hoop-wrapped jacketing system made of carbon fiber has less than 5% of the axial stiffness of steel, allowing greater lateral deflection under load and corresponding higher ductility while providing higher circumferential (hoop) strength [Norris, et al., 1997]. Carbon-composite retrofit wrapping is significantly more durable than steel jackets, by a factor of 2 to 4. In addition, carbon is unaffected by water or alkalis, and does not corrode. Carbon-composite retrofit wrapping, however, still involves many processes and is relatively expensive [Meier and Kaiser, 1991].

1.3 ADVANCED COMPOSITE REINFORCEMENT IN CONCRETE STRUCTURES

Advanced composites have been studied for many years in the aerospace industry as a high strength, high stiffness, and lightweight alternative to aluminum and steel. Due to the recent large-scale downsizing of military and aerospace programs in the United States, many researchers in these industries have begun to explore broader applications for modern materials known as advanced composites [Smart & Jensen, 1996]. The most common advanced composite materials are generally composed of high strength fibers such as carbon or fiberglass embedded in durable resins such as epoxies or polyesters. The term “advanced” applies to composite materials with a high fiber volume fraction which results in high strength and stiffness. These materials are capable of being primary load bearing components of a structure. In the case of reinforced concrete, the benefits of a lighter weight reinforcement does not significantly affect the overall weight of the structure. While the specific strength and stiffness do not in themselves warrant the use of composites, they are added benefits to a non-corrosive concrete reinforcement.

The use of composite materials in construction industry and infrastructure-related applications has greatly increased in recent years [Saadatmanesh, 1997]. Fiber Reinforced Plastics (FRPs) are generally constructed of high performance fibers such as carbon, aramid, or glass which are placed in a resin matrix. By selecting among the many available fibers, geometries and polymers, the mechanical and durability properties can be tailored for a particular application. This synthetic quality makes FRP a good choice for civil engineering applications as well [Norris, 1997]. Polymers, which include the resins used in in this research, have the advantages of low cost, ease of workability, and good resistance to environmental conditions. Although these materials are susceptible to damage due to ultra-violet rays, coatings have become available which will protect the fiber and resin when exposed to sunlight.

1.4 CONTAINMENT OF CONCRETE COLUMNS FOR SEISMIC CONSIDERATIONS

In the seismic design of reinforced columns for buildings and bridge substructures, the column reinforcement must be detailed for ductility in order to ensure that the shaking from large earthquakes will not cause collapse. Past tests have shown that the confinement of concrete by suitable arrangements of transverse reinforcement results in a significant increase in both strength and the ductility of compressed concrete. Mander and Priestley have developed stress-strain models for concrete subjected to uniaxial compressive loading and confined transverse reinforcement. The unconfined “cover concrete” will eventually become ineffective after the compressive strength is attained, but the core concrete will continue to carry stress at high strains. Their model shows that good confinement of the core concrete is essential if the column is to have a “reasonable plastic rotational capacity to maintain flexural strength” [Mander, et al., 1988a]. In general, the higher the axial compressive load on the column, the greater the amount of confining reinforcement necessary to achieve ductile performance. Therefore, the most important design consideration for ductility in plastic hinge regions is the provision of sufficient transverse reinforcement in order to confine the compressed concrete, to prevent buckling of the longitudinal bars, and also prevent shear failure.

Saadatmanesh also conducted a theoretical study on the behavior of confined reinforced concrete columns; however, in these studies they used high-strength fiber composite straps instead of steel reinforcement [Saadatmanesh, et al., 1997]. Both glass fiber reinforced plastic (GRFP) and carbon fiber reinforced plastic (CRFP) confining straps were investigated in a study to enhance strength and ductility of existing concrete columns. These “straps” were wrapped like a blanket in layers around a 915-mm (3-ft) diameter and 3.66-m (12-ft) height test column [Saadatmanesh, 1997]. The majority of the fabric fibers in the straps were unidirectionally arranged in the hoop direction and impregnated with the resin mixture during the fabrication process. Test results showed that the concrete compressive strength and strain increased substantially when it was wrapped with the composite straps. This was considered an effective technique for repairing earthquake-damaged columns; however, this method also has many drawbacks when considering the time and cost in preparing the column for repair. The repair procedure consisted of chipping out loose concrete in the failure zones, filling the gap with fresh concrete, inserting rubber spacers to the finished surface, and wrapping the composite straps on top of the spacers. The final step of the repair was pressure-injecting epoxy in the gap (provided

by the spacers) between the composite wraps and the concrete surface. One week was required in order for the fresh concrete and epoxy to cure before the repaired column could be tested.

1.5 PARTIAL CONTAINMENT VS. FULL CONTAINMENT

Most research in the area of strengthening reinforced concrete columns seems to be focused on the use of full containment in order to control the failure mode of the column when subjected to seismic loads. This research is unique in that the study focuses on using only partial containment to prevent these same failure modes. In existing reinforced concrete columns where insufficient transverse reinforcement is provided, three different types of failure modes can be observed under seismic loads. The first and most critical failure mode is shear failure where the rupture of transverse reinforcement can lead to explosive column failures (see Figure 5).

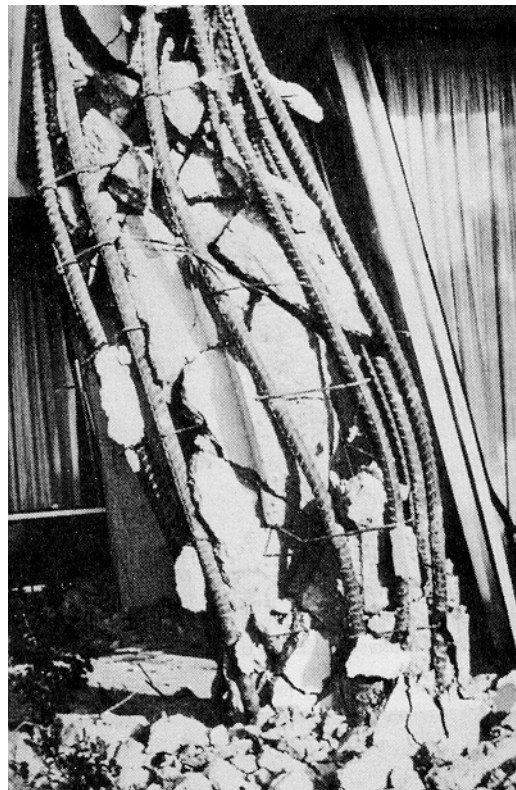


FIGURE 5 COLUMN FAILURE CAUSED BY LACK OF TRANSVERSE REINFORCEMENT

The second column failure mode consists of a confinement failure in the plastic hinge region of the column where the core concrete fails in compression. Finally, some bridge columns fail due to lap splices in the column reinforcement where debonding occurs between the steel reinforcement and concrete due to lack of confinement at the connection between the footing and the column. When considering the forces of an earthquake, none of these modes can be viewed separately since retrofitting for one deficiency may only shift the seismic problem to another location and failure mode [Seible, 1997]. However, costs in time and materials could be reduced considerably if a feasible method was developed to control these failure modes while only using partial containment. This thesis will focus on strengthening concrete columns in order to control shear failure and therefore subject these columns to axial compression only.

1.6 PROJECT OBJECTIVE

The objective of this research is to introduce novel concepts for advanced composite reinforcement in concrete columns in order to control shear failure due to axial compression. In order to accomplish this objective, this research encompasses a new methodology of reinforcing concrete columns with fiber-reinforced plastic composites. Reinforcement entails the use of grid structures composed of members that are placed circumferentially as well as longitudinally. This method of reinforcement is the first of its kind because it relies on partial containment using advanced composite members, yet it allows concrete columns to be subjected to greater compressive loads before induced shear failure occurs. Three generations of advanced composite structures were tested in axial compression in order to explore geometric configurations of the composite grid structures and optimize their strength. The first two generation grid structures focus on construction of new columns using composite reinforcement while the third generation columns were constructed with an application for existing columns. The testing performed in this research is a “proof of concept” and does not deal directly with retrofit and rehabilitation of existing steel reinforced columns. However, once the load-deflection behavior and load transfer mechanisms of composite grid reinforced concrete structures are understood a validated design criteria can be established. Such a design criteria will allow this methodology to be extended to the rehabilitation and seismic retrofit of existing concrete columns and piers in the future.

CHAPTER 2

EXPERIMENTAL APPROACH

Three different generations of grid structures were constructed and then tested in axial compression. These different generations were deemed necessary as more information was gained about the failure modes and different materials and geometric configurations were employed to increase the strength of the columns. The first and second generation columns consisted of constructing the reinforcement first and placing it inside the column for internal reinforcement (similar to steel rebar). However, the third generation column was used as external reinforcement to simulate a retrofit for an existing concrete column.

2.1 DESCRIPTION OF 1ST GENERATION COLUMNS

Column specimens 46 cm (18 in.) long with a 20 cm (8 in.) circular cross-section were chosen for convenience, since the longitudinal reinforcement was pre-cut to this length and the ratio of column diameter to column length is appropriate for axial compression tests. The concrete columns were reinforced with advanced composite grid structures containing both circumferential rings (circs) and longitudinal stiffeners (longis). The circs are 17.8 cm (7.1 in.) in diameter and contain a total of fifteen holes for connecting longis. The circs are composed of carbon fiber and vinyl ester resin that has been filament wound onto a mandrel and then sliced into 1.3 cm (0.5 in.) thick sections using a diamond bit band saw. The longitudinal reinforcement is composed of pultruded fiberglass rods. Different geometric configurations of the composite reinforcement were obtained by varying the number of longis and circs (see Figure 6). Two sets of six different geometric configurations were constructed using 5.1 cm (2.0 in.) and 10 cm (4.0 in.) spacing between circs, while varying the number of longis: 5, 10, and 15 (Figure 7).

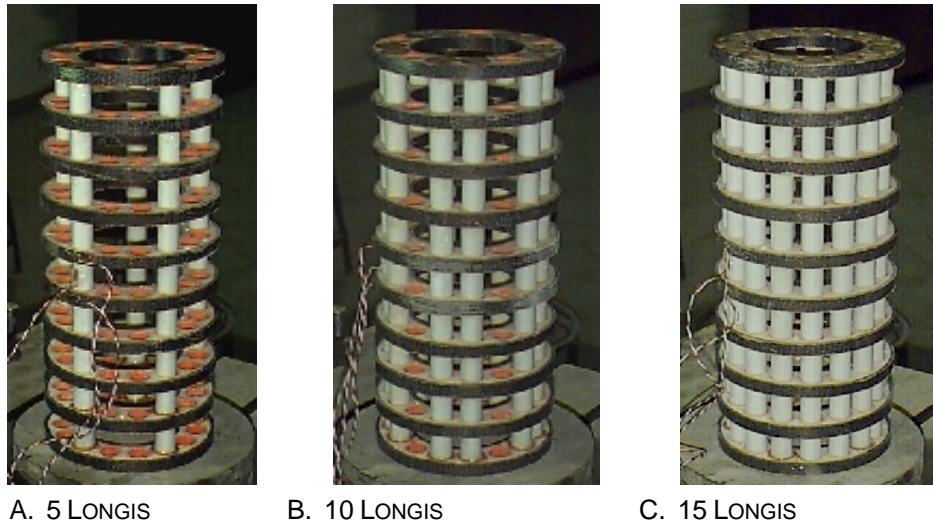


FIGURE 6 PHOTOGRAPHS OF 1ST GENERATION COLUMNS WITH 10 CIRCS, 5.1 CM (2.0 IN.) SPACING

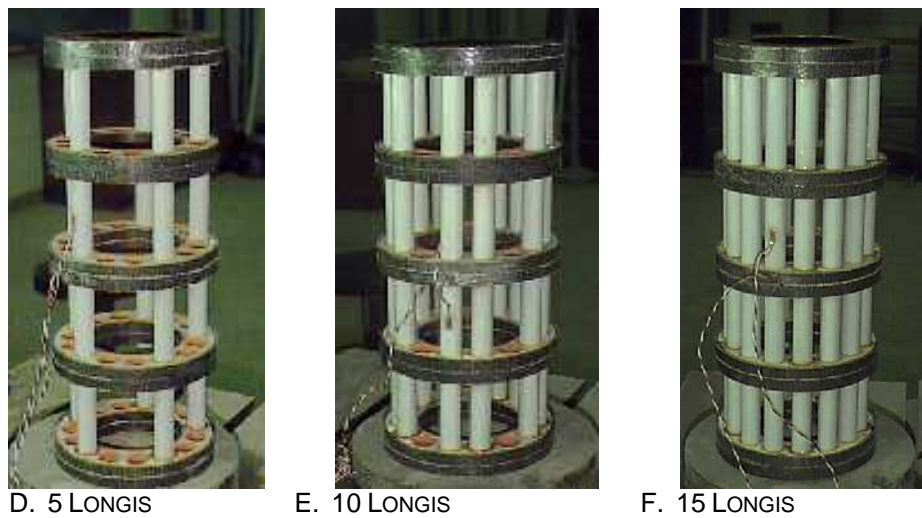


FIGURE 7 PHOTOGRAPHS OF 1ST GENERATION COLUMNS WITH 10 CIRCS, 10.2 CM (4.0 IN.) SPACING

A 20.3 cm (8.0 in.) diameter sono-tube (circular cardboard tube) was used as the mold for these columns in an effort to standardize these tests with industry as much as possible. Because of this large mold diameter, a layer of concrete approximately 1.3 cm (0.5 in.) covered the outer part of the composite grid structure. In order to fully demonstrate the role of the circs, a fully-packed column (15 longis) was constructed using only one circ on each end for a total spacing between circumferential reinforcement of 46 cm (18.0 in.).

2.2 DESCRIPTION OF 2ND GENERATION COLUMNS

The second generation columns contain the same longitudinal reinforcement as the first generation columns; however, the diameter is 20.6 cm (8.13 in.) allowing for a total of 21 longis. Also, a higher quality carbon fiber was used during the winding process resulting in a much stronger circ. Due to limited materials, only four second generation grid structures were constructed, each with a different geometric configuration. Grid structures were built using 6.4 cm (2.5 in.), 7.6 cm (3.0 in.), 8.9 cm (3.5 in.), and 46 cm (18.0 in.) spacing between second generation circs with 21 longis in each column (see Figure 8). This last configuration was used to demonstrate the role of the circs in axial compression and compare with the test matrix of the first generation columns. The larger diameter of the second generation circ permitted sections of the tubular cardboard molds to be used as spacers while remaining flush on the outside with the circs. This reduced the layer of concrete cover on the outside of the composite grid structure and increased the volume of contained concrete compared to the first generation columns.



G. 6 CIRCS



H. 7 CIRCS



I. 8 CIRCS

FIGURE 8 PHOTOGRAPHS OF 2ND GENERATION COLUMNS WITH 21 LONGIS, VARIED SPACING OF CIRCS

2.3 DESCRIPTION OF 3RD GENERATION COLUMNS

Although the third generation columns were constructed in a different manner than the first two generations, the use of composite longitudinal and circumferential reinforcement employed is very similar. This column has a diameter of 23 cm (9.0 in.) and a length of 52 cm (20.5 in.) which is the same diameter to column ratio as the first and second generation columns. The longitudinal reinforcement in these columns was composed of a hybrid of fiberglass and graphite while the circs were composed of nominal tensile modulus fiberglass “bands.” A total of 18 longis were used while the number of 10.2 cm (4.0 in.) bands varied from partial to full containment. This allowed for containment of 40, 80, and 100 percent (see Figure 9).

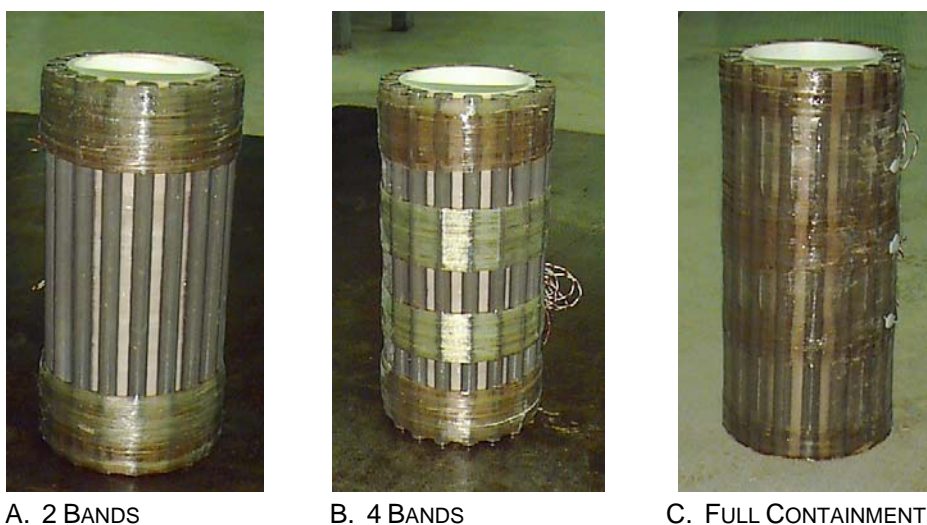


FIGURE 9 PHOTOGRAPH OF 3RD GENERATION COLUMNS, WITH 40, 80, & 100% CONTAINMENT

2.4 THE TEST MATRIX

The test matrix is composed of thirty concrete columns and employs three generations of composite grid structures. Thirteen of these columns were constructed using first generation circs, four with second generation columns, and eight with third generation columns (see Figure 10). The remaining five columns were used as control specimens for comparison with the composite reinforced columns. The number of columns was limited by the amount of materials available; therefore, the test matrix was organized so that axial compression tests would cover a

spectrum of circ-longi combinations. This approach allowed for a comparison between different composite grid structures in order to optimize the strength of the columns (see Tables 1 & 2).

FIGURE 10 TEST MATRIX

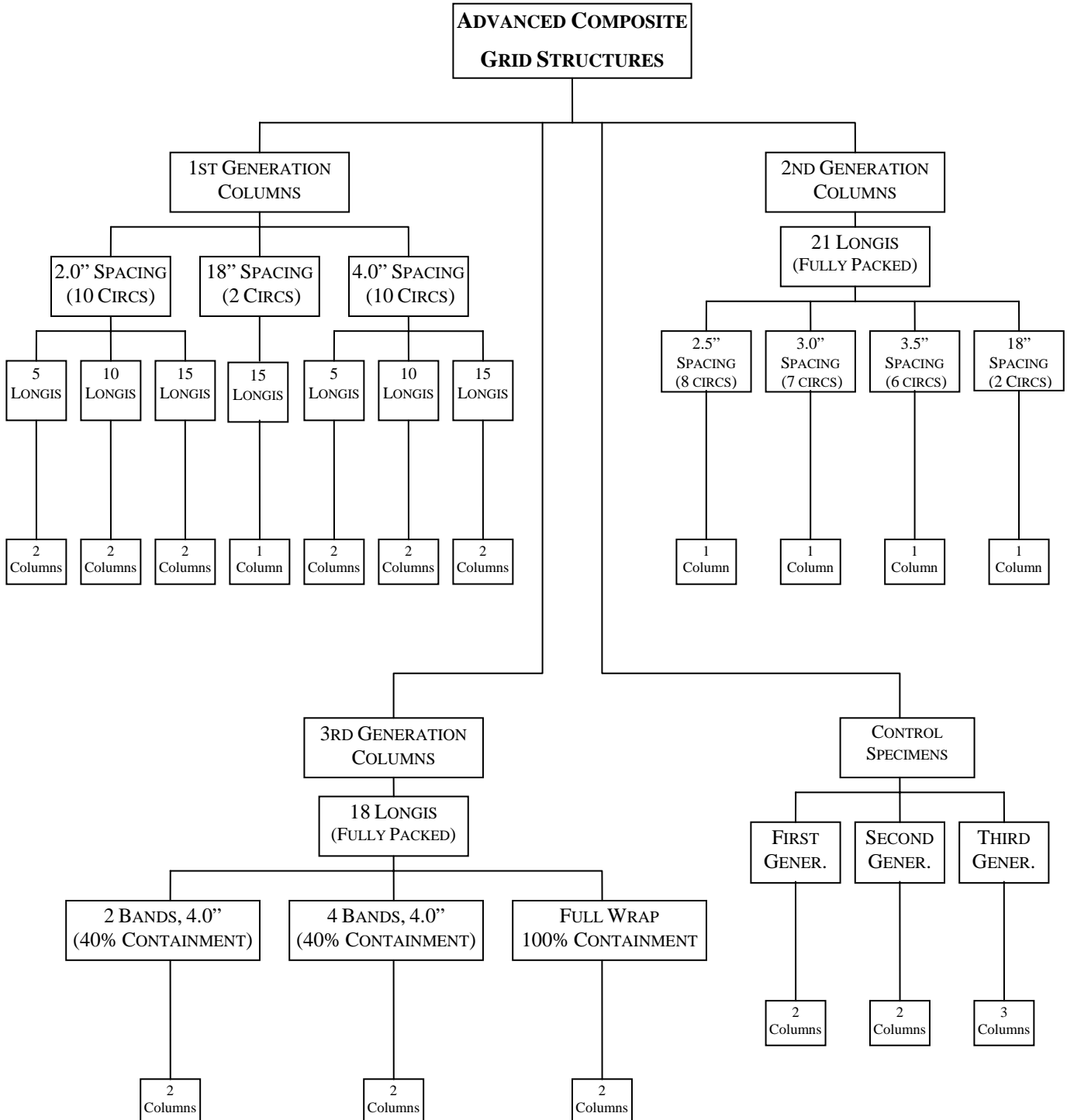


TABLE 1 1ST AND 2ND GENERATION ADVANCED COMPOSITE GEOMETRIC CONFIGURATIONS

Column Generation	Column ID	Number of Circs	Spacing [cm (in)]	Number of Longis	Aggregate Size [cm (in)]
1st	A1	10	5.1 (2.0)	5	6.4 (0.25)
	A2	10	5.1 (2.0)	5	6.4 (0.25)
	B1	10	5.1 (2.0)	10	6.4 (0.25)
	B2	10	5.1 (2.0)	10	6.4 (0.25)
	C1	10	5.1 (2.0)	15	6.4 (0.25)
	C2	10	5.1 (2.0)	15	6.4 (0.25)
1st	D1	10	10.2 (4.0)	5	6.4 (0.25)
	D2	10	10.2 (4.0)	5	6.4 (0.25)
	E1	10	10.2 (4.0)	10	6.4 (0.25)
	E2	10	10.2 (4.0)	10	6.4 (0.25)
	F1	10	10.2 (4.0)	15	6.4 (0.25)
	F2	10	10.2 (4.0)	15	6.4 (0.25)
2nd	G	6	6.4 (2.5)	21	9.5 (0.375)
	H	7	7.6 (3.0)	21	9.5 (0.375)
	I	8	8.9 (3.5)	21	9.5 (0.375)
1st	O	2	46 (18.0)	15	6.4 (0.25)
2nd	J	2	46 (18.0)	21	9.5 (0.375)
Control Specimens	K				6.4 (0.25)
	M1				9.5 (0.375)
	M2				9.5 (0.375)

TABLE 2 3RD GENERATION ADVANCED COMPOSITE GEOMETRIC CONFIGURATION

Column Generation	Column ID	Number of Bands	Band Width [cm (in)]	Amount of Containment	Aggregate Size [cm (in)]
3rd	A1	2	10.2 (4.0)	40%	9.5 (0.375)
	A2	2	10.2 (4.0)	40%	9.5 (0.375)
	B1	4	10.2 (4.0)	80%	9.5 (0.375)
	B2	4	10.2 (4.0)	80%	9.5 (0.375)
	C1	Full	51.0 (20.0)	100%	9.5 (0.375)
	C2	Full	51.0 (20.0)	100%	9.5 (0.375)
Control Specimens	D1				9.5 (0.375)
	D2				9.5 (0.375)

CHAPTER 3

COMPOSITE GRID MANUFACTURE

3.1 1ST AND 2ND GENERATION GRID MANUFACTURING

The manufacturing process for these advanced composite grids utilize some of the most efficient processing techniques that are currently available: filament winding and pultrusion. The circs are composed of two hoop wound rings separated by extruded polymer tubes. The tubes are bonded to carbon fiber rings by vacuum infiltrated epoxy (see Figure 11).



FIGURE 11 PHOTOGRAPH OF END CIRCS FOR 1ST AND 2ND GENERATION COLUMNS

The epoxy secures the 15 or 21 extruded polymer rings (depending on the circ generation) for later insertion of the longis. The longis are pultruded with a high fiber volume fraction to resist flexure while the circs resist the radial expansion of the concrete under axial compression. The composite grid structure is constructed by running longis through the extruded polymer rings with

the appropriate spacing. For the 1st generation columns, a drop of five-minute epoxy was used to bond each of the circs to the longis at right angles. For the 2nd generation longis, however, only the end circs were bonded. The middle circs were spaced with sections of cardboard tube, which were sealed to the circs using a caulking compound. The tubular cardboard mold and caulk were removed after the concrete cured. Once the grid structure composed of both graphite circs and fiberglass longis was embedded in concrete, it acted as one reinforcement structure under axial load.

3.2 3RD GENERATION GRID MANUFACTURING

While the first and second generation columns were manufactured as a means for internal reinforcement, this 3rd generation of grid structure was manufactured with existing concrete columns in mind. A 15.3 cm (6 in.) diameter Polyvinyl Chloride (PVC) tube was used for a mandrel and two layers of Pittsburg Plate Glass, Mandeville Co. nominal tensile modulus (10.5×10^6 psi) strand fiberglass were wound around the PVC along the full length of the column. Before the resin cured, 18 longis were equally spaced around the column and the new grid was again wound on the filament winder (see Figure 12).



FIGURE 12 PHOTOGRAPH OF 3RD GENERATION COLUMN (ENDVIEW)

This fiberglass was combined with a resin composed of Derakane 8084 epoxy vinyl ester, Cobalt Napthenate, Trigonox 239A, and 2,4-Pentanedione. Derakane 8084 resin is an elastomer modified epoxy vinyl ester that expands the serviceability of thermoset resins in traditional fiber reinforced plastic (FRP) applications. This particular type of resin offers increased adhesive strength, superior resistance to abrasion and triple the toughness performance of standard epoxy vinyl ester resins [Dow Chemical Company]. The Cobalt Napthenate acts as a promoter and the 2,4-Pentanedione acts as a retarder while the Trigonox eliminates the foam that is usually a problem in civil applications which use vinyl ester resins. This second winding involved 4 layers in order to create the “bands” and full-containment as shown in Figure 13. Two separate columns were also constructed using only the PVC and initial 2 layers of filament wound fiberglass (see Figure 13). These columns were constructed in order to demonstrate the need for longitudinal reinforcement and additional containment.

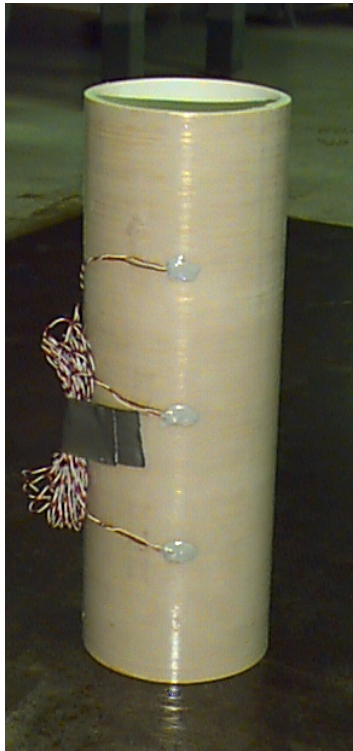


FIGURE 13 PHOTOGRAPH OF PVC WITH 2 LAYERS OF FIBERGLASS

3.3 STRAIN GAGE PLACEMENT

A preliminary compression test was performed on a single 1st generation composite grid structure without any concrete. Twelve electrical resistance gages were mounted on the circs and longis in order to determine the critical locations for stress and the resultant strain (see Figure 14).

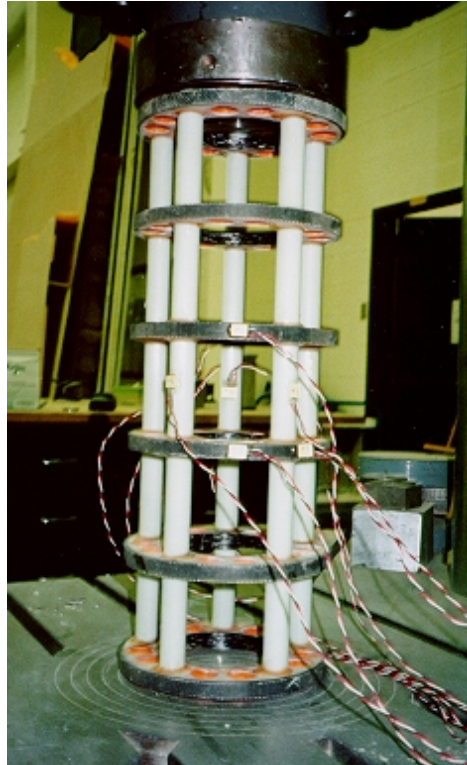


FIGURE 14 PHOTOGRAPH OF STRAIN GAGE PLACEMENT TEST

For the columns involved in this research, at least one pair of electrical resistance strain gages were mounted in each column before the concrete was poured. The strain gages were placed on the longitudinal reinforcement at the mid span of the longi and on the outside of the middle circ or “band.” As many as 6 gages were used on the 2nd generation columns. The mounting of the strain gages followed the manufacturers suggested procedure. The surface was prepared through degreasing, surface abrasion, and conditioning. The strain gage was mounted with a small amount of five-minute epoxy. Pressure was applied to the gage as the epoxy cured to insure a good bond. Lead wires were then soldered to the tabs and the gages were checked with a strain indicator box to insure that they were functioning properly. The completed gage was covered with epoxy to protect it while the concrete was placed and cured.

CHAPTER 4

CONCRETE COLUMN MANUFACTURE

4.1 MIX DESIGN

A mix design corresponding to a compressive strength of 20.7 MPa (3 ksi) was chosen for 1st and 2nd generation columns. Although an even higher strength is common for reinforced concrete structural members, this low strength mix was used to illustrate the effectiveness of the composite grid and also to ensure that the maximum load of the compression machine, 1.3 MN (300 kip), would not be exceeded. Because of the synergistic relationship between the composite grid reinforcement and the concrete, the ultimate strength of these columns did exceed the compression machine capacity. Consequently, a compression machine of 17.8 MN (4,000 kip) was used for testing and a concrete mix with a compressive strength of 34.5 MPa (5 ksi) was used for the 3rd generation columns to demonstrate the column's full potential in axial compression (see Table 3). Appendix A contains more information on the material characteristics and volumes of aggregate and cement used in this mix design.

TABLE 3 CONCRETE MIX DESIGN

Compressive Strength	20.7 MPa (3 ksi)	34.5 MPa (5 ksi)
Portland Cement	Type I	Type III
Max Aggregate Size	1.0 cm (0.375 in)	1.3 cm (0.50 in)
Water	10.2%	8.5%
Portland Cement	15.6%	17.2%
Coarse Aggregate	43.0%	43.0%
Fine Aggregate	31.2%	31.3%
Water/Cement ratio	0.65	0.49

4.2 PLACEMENT OF CONCRETE

The 1st and 2nd generation columns were formed using Rocky Mountain concrete sonotubes[®] (see Figure 15); however, the 3rd generation column used the PVC mandrel to contain the interior concrete. Prior to pouring the concrete, the sonotubes were cut and sanded to a length of 50.8 cm (20 in.) and a steel base plate was coated with a release oil. Small holes were drilled in the sonotubes to allow the strain gage wires to exit the column molds. The composite grid structure was centered in the middle of the sonotube while standing up-right. The concrete was mixed in a large portable mixer and the sonotubes were filled with concrete in five lifts, each approximately 10 cm (4 in.) in height. Each lift was rodded 50 times with a blunt rounded rod and the molds were struck sharply 5 times with a mallet. An aggregate of 0.64 cm (0.25 in.) diameter was used with first generation columns and an aggregate of 1.0 cm (0.375 in.) diameter was used with the second and third generation columns in order to insure the placement of concrete between the longitudinal reinforcement.

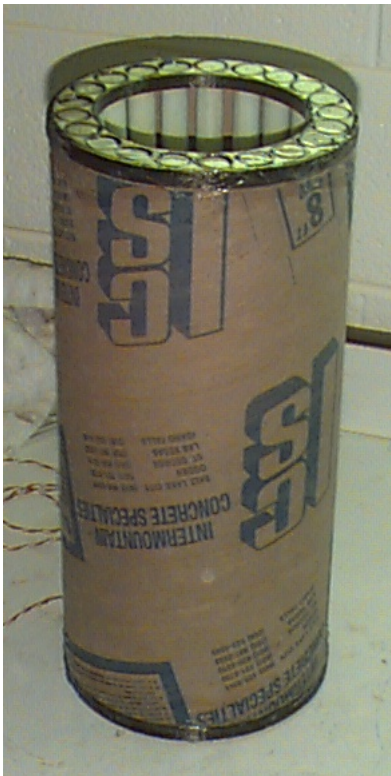


FIGURE 15 SONOTUBE[®] USED TO SPACE CIRCS

4.3 CONTROL SPECIMENS

A 20.3 cm (8.0 in.) diameter by 45.7 cm (18 in.) long compression cylinder was poured with each set of 1st and 2nd generation columns (two sets). These sets or batches of the same mix design were required because of the limited capacity of the portable mixer. These full-scale specimens were used as control specimens in order to compare failure modes and compression strengths. The third generation column used smaller 15.2 cm (6 in.) control specimens to determine the compression strength of the mix design. Similar to the other columns, these control specimens were filled in five lifts of equal height and each lift was rodded 50 times. These samples were tested at the same time as the composite grid reinforced columns in order to determine the concrete strength at the time of testing (see Figure 16).



FIGURE 16 CONTROL SPECIMENS FOR 3RD GENERATION COLUMNS – 6 INCH DIAMETER

4.4 CURING

The 1st and 2nd generation columns as well as the control specimens were left in the sono-tube molds overnight. The next day the sono-tube mold was removed from the columns and the concrete specimens were placed in the fog room where the temperature was maintained at approximately 23.9 °C (75 °F) and 90-95% humidity. The 1st and 2nd generation columns cured in the fog room for 28 days, while the the 3rd generation columns cured for only 7 days due to the different type of Portland cement used in the mix design (see Figure 17).



FIGURE 17 3RD GENERATION OLUMNS AFTER BEING POUED

CHAPTER 5

TEST FIXTURE SETUP

5.1 OVERVIEW OF TEST FIXTURE SETUP

The preliminary compression test of the single composite grid structure (with and without concrete) was performed on a 1.3 MN (300 kip) Baldwin compression machine. The entire load head was allowed to swivel in order to ensure an evenly distributed load. Because the load required to fail this column (with reinforcement – 6 circs, 5 longis) almost exceeded the load capacity of this machine, the 1st and 2nd generation columns were tested in Denver, Colorado at the Department of Interior’s Bureau of Reclamation. This facility has a 17.8 MN (4,000 kip) and 22.2 MN (5,000 kip) Baldwin test machines (see Figure 18). The 17.8 MN compression machine was used to fail the 1st, 2nd, and 3rd generation columns in axial compression.

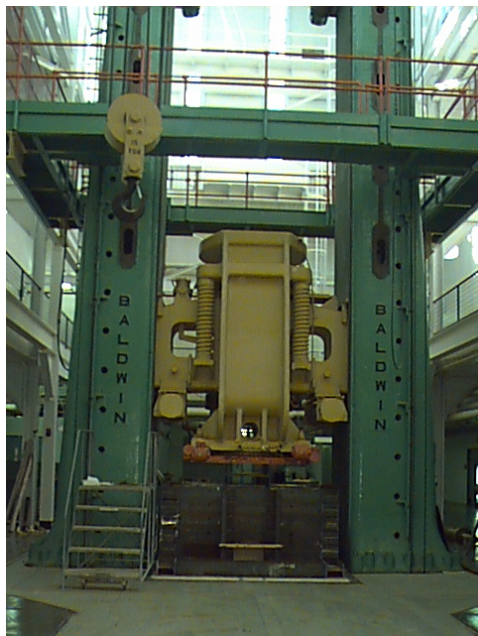


FIGURE 18 5,000 KIP BALDWIN COMPRESSION MACHINE

5.2 DESIGN AND FABRICATION OF SULFUR ENDCAPS

After the concrete columns had been allowed to cure, they were capped using a sulfur compound. A sulfur cap ensures that the load will be distributed over the entire end of the column. This was important considering the configuration of composite reinforcement. Sulfur compound is commonly available as a powder or solid “chips” that must be heated over 250 °F before it will melt into a liquid. Once in liquid form, the sulfur is poured into a mold, and the concrete specimen is placed on top of the mold (see Figure 19).



FIGURE 19 PHOTOGRAPH OF 1ST GENERATION COLUMNS WITH SULFUR ENDCAPS

Because of the unusual diameter of the column, an aluminum mold was designed and built in order to more effectively cap the ends of each column (see Appendix B). The compressive strength of the sulfur compound used in this research was approximately 41.4 MPa (6 ksi). When the loads exceeded this value, the sulfur cap crumbled reducing its efficiency. A higher strength sulfur compound of 82.7 MPa (12 ksi) was used for the third generation columns. Even with this high strength compound, many of these 3rd generation columns exceeded this load and pulverized the sulfur endcap in the process (see Figure 19). The steel endcaps contained this failure and the sulfur compound was able to fulfill its function.

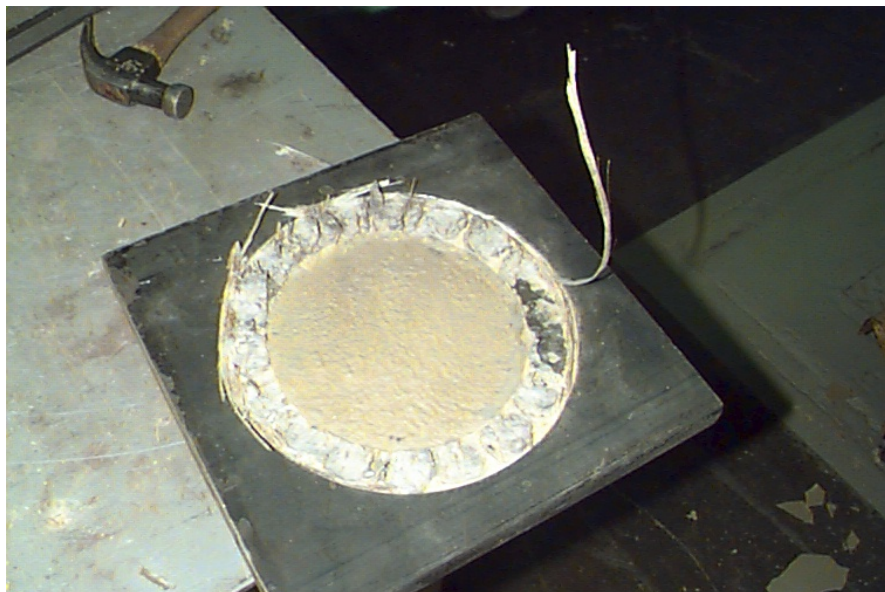


FIGURE 20 PULVERIZED SULFUR CAPPING INSIDE OF STEEL ENDPLATE

5.3 DESIGN AND FABRICATION OF STEEL ENDCAPS

Because of this end failure, steel endcaps were also designed and manufactured for use with the 3rd generation columns (see Figure 21). These endcaps prevented brooming of the longis and had a significant effect on the overall strength and failure mode as discussed in Chapter 6.



FIGURE 21 3RD GENERATION COLUMN WITH STEEL ENDCAPS

CHAPTER 6

EXPERIMENTAL PROCEDURE

6.1 TEST SPECIMEN PREPARATION

After removal from the fog room, the concrete columns were allowed to dry until the surface was free of excess moisture. Strain gages were checked with the strain indicator box and marked with colored tape to identify leads to longitudinal and circumferential strain gages. Each column was then identified with a tag and packaged in 25 by 30 by 56 cm (10" by 12" by 22") cardboard boxes for the 500 mile trip to Denver, Colorado (see Figure 22). Wet papertowels were wrapped around the columns to keep them moist and foam packaging was used to protect the endcaps on the columns during transport.



FIGURE 22 1ST AND 2ND GENERATION COLUMNS PACKAGED FOR TRANSPORT

6.2 DATA ACQUISITION

For preliminary tests at Brigham Young University, data was acquired on a Compaq® Deskpro XL 566 with an Adaptec® 154CF SCSI Controller. This controller used an HPIB interface to communicate with a NEFF® 470 system containing twelve 4-channel bridge conditioning cards for strain gage and load cell data and one 16-channel differential input card for measuring changes in DC voltage inputs. The system employed Autonet 4.11® operating system. For compression tests conducted on all other grid structures, data was acquired on a portable Optim Electronics Megadeck® 5414AC with a 16-bit analog digital converter (see Figure 23).



FIGURE 23 PHOTOGRAPH OF MEGADECK® DATA ACQUISITION SYSTEM

Because these systems were portable, the distance between the data acquisition system and the test specimen was less than 6 m (20 ft.). This allowed the instrument leads to be relatively short. Thus, a two-wire scheme was used to simplify connection of the strain gages. Because of the high compression load sustained by the columns during testing, the data acquisition system and personnel were protected by plexi-glass shields (see Figure 24). These shields proved to be vital for safety during testing due to the explosive nature of the outer layer of concrete on the columns during failure.



FIGURE 24 PLEXI-GLASS SHIELDS USED FOR PROTECTION DURING TESTING

6.3 SPECIMEN TESTING

Once the strain gage leads and standard Linear Variable Differential Transformer (LVDT) were connected, the data acquisition was started and the swivel load head was lowered until contact was made with the top of the column. The range of the Baldwin compression machine was set to the “low” range (0-25%) and the load dial was zeroed. The hydraulics were then started and load was applied to the column at a constant rate of ~900-1300 N/sec (200–300 lbs/sec). The loading rate varied somewhat between specimens because of the manual controls on the compression machine. The compression load was increased steadily until initial cracking of the column occurred. For the 1st generation columns this was when the load reached approximately 1.3 MN (300 kips). A slight drop in load indicated the initiation of cracking. This was followed by separation of the outer layer of concrete in the form of high velocity projectiles. After this initial failure the load continued to climb steadily until a sudden failure initiated at one end of the column. Plain concrete columns typically fail in shear, as evidenced by the 45° to 60° angle cracks after failure. This type of failure is shown in the control specimens used to

determine the compressive strength of the concrete mix design for the 1st and 2nd generation (see Figure 25)



FIGURE 25 PHOTOGRAPH OF CONTROL SPECIMEN AFTER FAILURE

In the advanced composite grid reinforced concrete columns, failure generally initiated at one end of the column instead of the typical shear failure mode. The concrete crumbled locally, the end circ slid down the longis and the ends of the pultruded longis exhibited brooming (see Figure 26).



FIGURE 26 PHOTOGRAPH OF TYPICAL END FAILURE FOR 1ST GENERATION COLUMN

Eventually the end circ would fail dramatically, sending the crumbling concrete flying away from the column, allowing further bending and brooming of the longis. At this point, the load on the column dropped by 1/3 to 1/2 and then slowly climbed back up to approximately the original maximum load level, and another circ would fail in a similar manner (see Figure 27). The second generation columns demonstrated similar behavior during failure but at a much higher load. Once two or three of these circs had failed the sustained compressive load would decrease significantly and the test was stopped.



FIGURE 27 CONTINUATION OF END FAILURE FOR 1ST GENERATION

CHAPTER 7

EXPERIMENTAL RESULTS

7.1 DATA REDUCTION PROCEDURE

During testing the data was stored automatically by the Optim Megadeck[®] operating system and later exported to the DOS[®] accessible drive as an ANSI[®] text file. The files were then read into Excel[®] spreadsheets. All of the data reduction was performed using Excel workbooks and the Excel Visual Basic[®] macro language. The initial data reduction involved removing unnecessary data points that were logged during the space of time between the initiation of data acquisition and the actual commencement of loading. The excess data at the end of the file was also removed. Slight variations in the strain starting point were compensated by zeroing the strain data with respect to initial readings. Also, macros written in Visual Basic were used to average and reduce excessive data for a specific test. Finally, load vs time, load vs total deflection, and stress vs strain graphs were generated in order to compare the behavior of the different composite grid configurations.

7.2 FIRST GENERATION COLUMNS WITH 5.1 CM SPACING

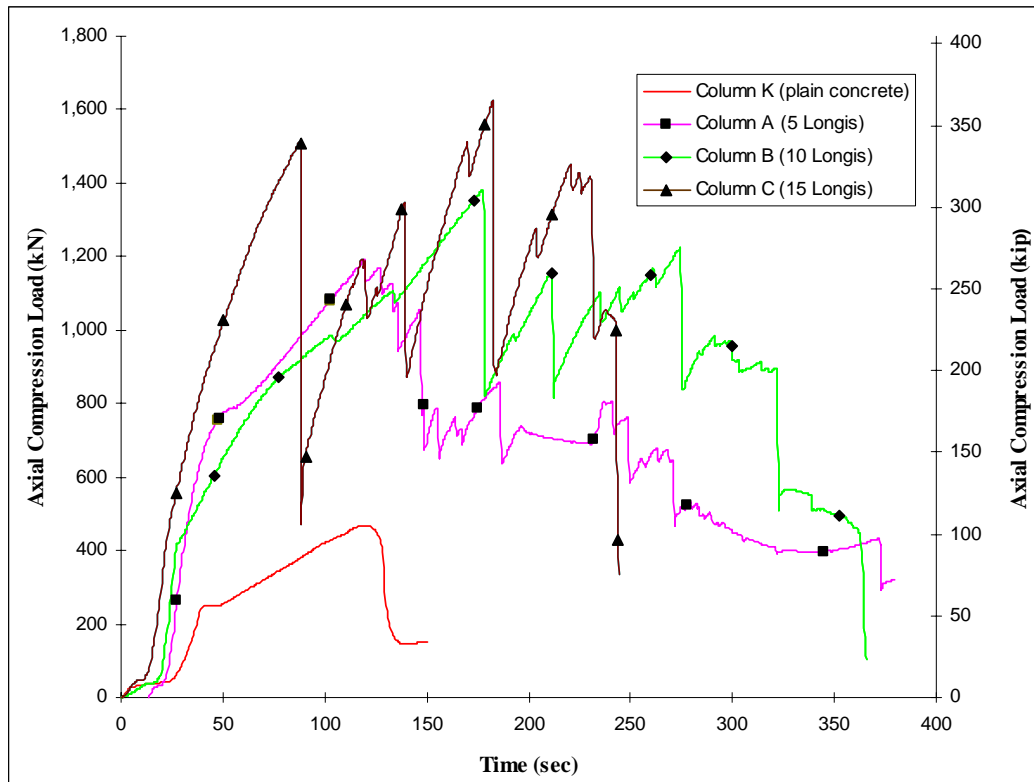
Columns A, B, and C consisted of 10 circles spaced 5.1 cm (2.0 in.) apart - from center to center of each circle - with the number of longis being varied 5, 10, and 15 respectively. The plain concrete (Column K) failed at 534 kN (120 kip) or 14.4 MN (2.1 ksi) while the 1st generation reinforced columns failed around 1334 kN (300 kip) or 40.7 MN. This is an improvement in axial strength by a factor of 2.8. The number of longis made a slight difference in the ultimate strength of the columns (see Table 4).

TABLE 4 COMPARISON OF 1ST GENERATION COLUMNS WITH 5.1 CM (2.0") SPACING

Column Generation	Column ID	Number of Cirs	Spacing [cm (in)]	Number of Longis	Aggregate Size [cm (in)]	Ultimate Load [kN (kip)]	Average [kN (kip)]
1st	A1	10	5.1 (2.0)	5	6.4 (0.25)	1,191 (268)	1,226 (276)
	A2	10	5.1 (2.0)	5	6.4 (0.25)	1,260 (283)	
	B1	10	5.1 (2.0)	10	6.4 (0.25)	1,274 (287)	1,328 (299)
	B2	10	5.1 (2.0)	10	6.4 (0.25)	1,381 (310)	
	C1	10	5.1 (2.0)	15	6.4 (0.25)	1,253 (282)	1,382 (311)
	C2	10	5.1 (2.0)	15	6.4 (0.25)	1,510 (340)	
Plain	K		5.1 (2.0)		6.4 (0.25)	468 (105)	468 (105)

An additional five longis increased the axial compressive strength of the columns by approximately 77.8 kN (17.5 kip) or 5.8%. This was expected because the modulus of fiberglass is much higher than that of concrete (10.7×10^3 ksi vs 3.1×10^3 ksi).

One of the most fascinating results from this research comes from load data recorded over time as the columns failed in compression. Because the load is controlled by the stroke of the compression machine, the load vs time graph can not be used to directly compare the columns. However, a comparison of load vs time shows how individual columns were affected as each circ failed (see Figure 28).

**FIGURE 28** LOAD VS TIME FOR 1ST GENERATION COLUMNS WITH 5.1 CM (2.0 IN.) SPACING

Although the strength of the individual columns was not affected a great deal by the number of longis, the load defelction curves were. The initial slope of the stress-strain curve is affected by properties of the fiberglass rods which are much stiffer than concrete (see Figure 29).

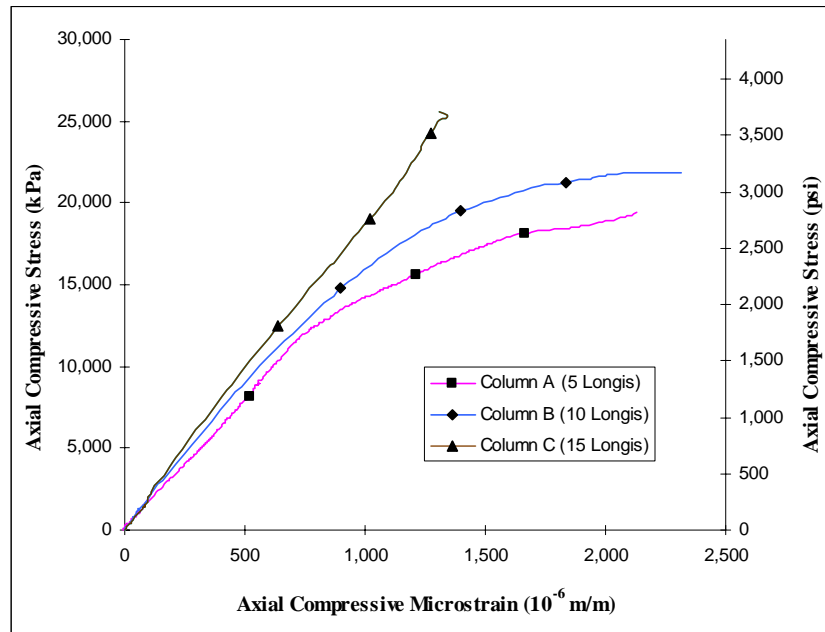


FIGURE 29 AXIAL STRESS VERSUS STRAIN FOR 5.1 CM SPACED 1ST GENERATION

This effect upon stress-strain curves in longitudinal reinforcement is also seen in the stress-strain relationship for the circumferential reinforcement (see Figure 30).

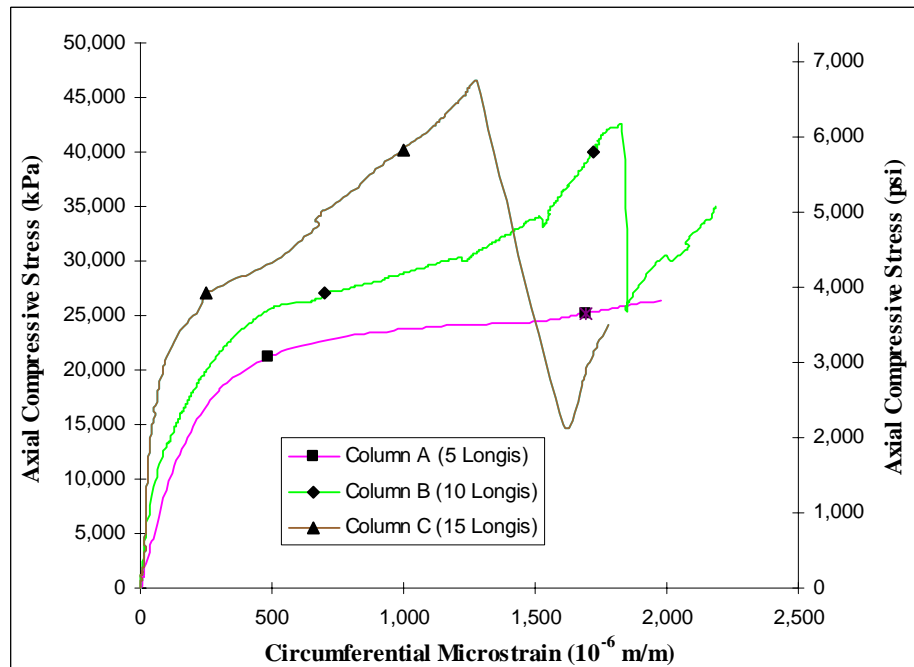


FIGURE 30 CIRCUMFERENTIAL STRESS VERSUS STRAIN FOR 5.1 CM SPACED 1ST GENERATION

Figure 30 shows that the initial slope of the stress-strain diagram for the circumferential reinforcement of the column is affected by the number of longis resisting flexure. As the first circ failed, the stress dropped dramatically and the strain increased for the remaining circs in the column. Typically, one would expect the strain to decrease as the stress dropped; however, this occurrence is likely due to the stroke control of the compression machine, coupled with the radial expansion of the columns.

7.3 FIRST GENERATION COLUMNS WITH 10.2 CM SPACING

Columns D, E, and F consisted of 10 circs spaced 10.2 cm (4.0 in.) apart - from center to center of each doubled circ - with the number of longis being 5, 10, and 15 respectively (see Figure 7). These composite grid structures were built in this configuration in order to see the effect of doubling the density of the first generation circs by placing two circs at each location while keeping the percentage of circumferential containment constant. The ultimate and average compressive loads are listed in Table 5.

TABLE 5 COMPARISON OF 1ST GENERATION COLUMNS WITH 10.2 CM (4.0") SPACING

Column Generation	Column ID	Number of Circs	Spacing [cm (in)]	Number of Longis	Aggregate Size [cm (in)]	Ultimate Load [kN (kip)]	Average [kN (kip)]
1st	D1	10	10.2 (4.0)	5	6.4 (0.25)	980 (220)	876 (197)
	D2	10	10.2 (4.0)	5	6.4 (0.25)	771 (173)	
	E1	10	10.2 (4.0)	10	6.4 (0.25)	1086 (244)	
	E2	10	10.2 (4.0)	10	6.4 (0.25)	1086 (244)	
	F1	10	10.2 (4.0)	15	6.4 (0.25)	1374 (309)	
	F2	10	10.2 (4.0)	15	6.4 (0.25)	1157 (260)	
Plain	K				6.4 (0.25)	468 (105)	468 (105)

The control specimen for these columns failed at 468 kN (105 kip) or 14.5 MPa (2.1 ksi) while the 10.2 cm (4.0 in.) spaced fiber reinforced columns failed around 1,070 kN (240 kip) or 34.5 MPa. This is an improvement in strength by a factor of approximately 2.3. The number of longis made more of a difference in the ultimate strength of these 10.2 cm spaced fiber-reinforced columns compared to the 5.1 cm spaced 1st generation columns (see Figure 32). An additional five longis increased the axial compressive strength of the columns by approximately 196 kN (44 kip) or 17.5%. These tests proved that doubling the density of the circs by spacing them closer together (5.1 cm vs. 10.2 cm apart) was more effective than doubling the density of the circs by spacing two circs at each location, 10.2 (4.0 in.) apart.

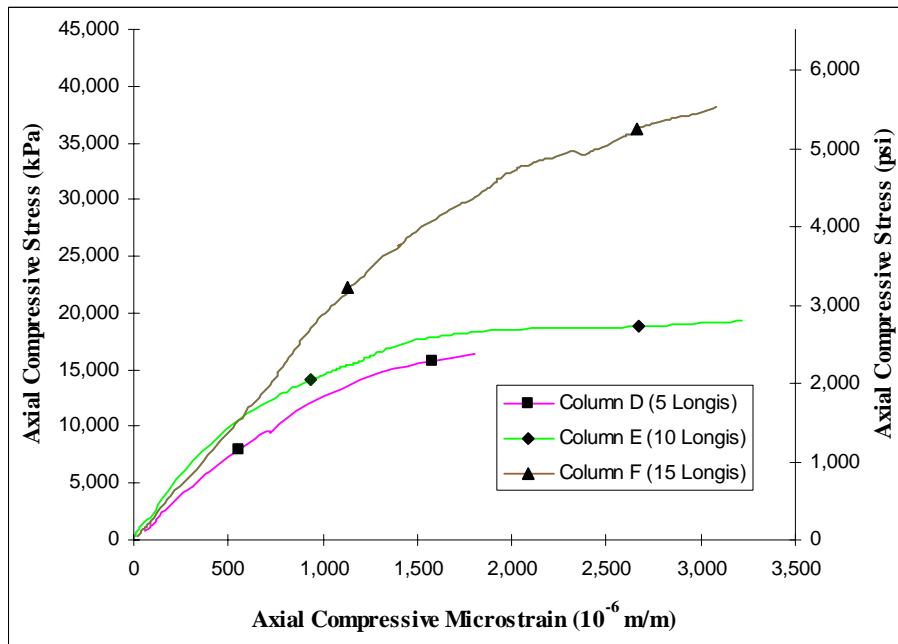


FIGURE 32 LONGITUDINAL STRESS VERSUS STRAIN FOR 10.2 CM SPACED 1ST GENERATION

The number of longitudinal reinforcement bars in the 10.2 cm (4.0 in.) spaced columns had a fair impact on the stress-strain curves. Most of the gages inside of the first generation columns failed to function very long due to an increase in strain after the first circ failed. However, Column F in Figure 32 shows the load transfer on a middle circ as several end circs failed in succession.

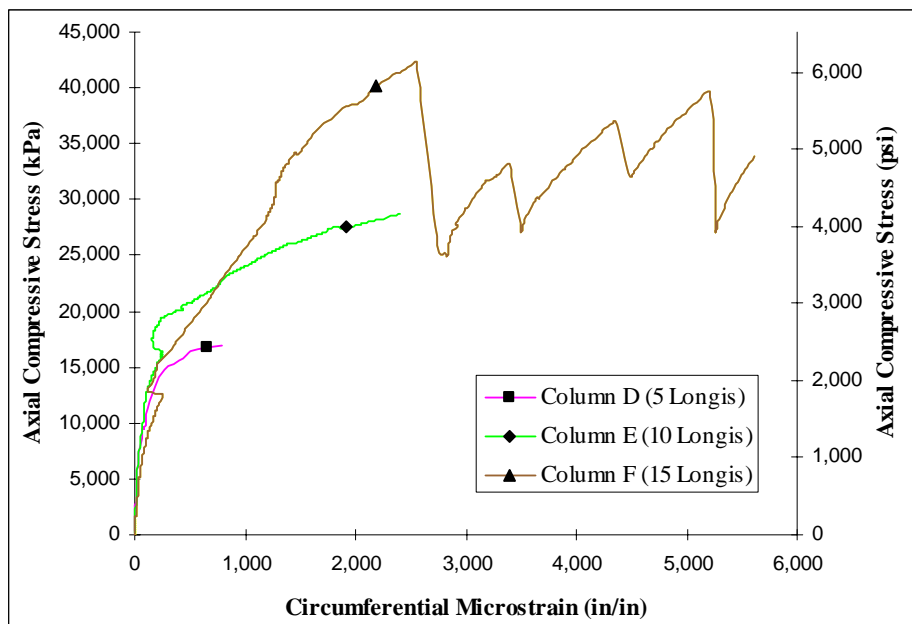


FIGURE 31 CIRCUMFERENTIAL STRESS VERSUS STRAIN FOR 10.2 CM SPACED 1ST GENERATION

7.4 SECOND GENERATION COLUMNS

The second generation columns were far superior in ultimate compressive strength when compared to the first generation. This was due to the higher quality of the carbon fiber hoop windings, not the additional number of longis (see Table 6).

TABLE 6 COMPARISON OF 2ND GENERATION COLUMNS

Column Generation	Column ID	Number of Circs	Spacing [cm (in)]	Number of Longis	Aggregate Size [cm (in)]	Ultimate Load [kN (kip)]
2nd	G	6	6.4 (2.5)	21	9.5 (0.375)	2,965 (667)
	H	7	7.6 (3.0)	21	9.5 (0.375)	3,190 (717)
	I	8	8.9 (3.5)	21	9.5 (0.375)	3,346 (752)
	J	2	46 (18.0)	21	9.5 (0.375)	1,220 (274)
Plain	M1				9.5 (0.375)	571 (128)

These columns were averaging around 3.15 MN (700 kip) or 97.2 Mpa (14.1 ksi) while the control samples for this generation had an ultimate axial compression strength of 569 kN (128 kip) or 17.1 Mpa (2.5 ksi). This shows an increase in strength by a factor of approximately 5.5. Although the second generation columns failed at three times the load of the first generation columns, their behavior was very similar. The load-time history for Column H is a typical example of this generation and its ability to repeatedly release stress through failure of a circ and then build up to even a higher load (see Figure 33).

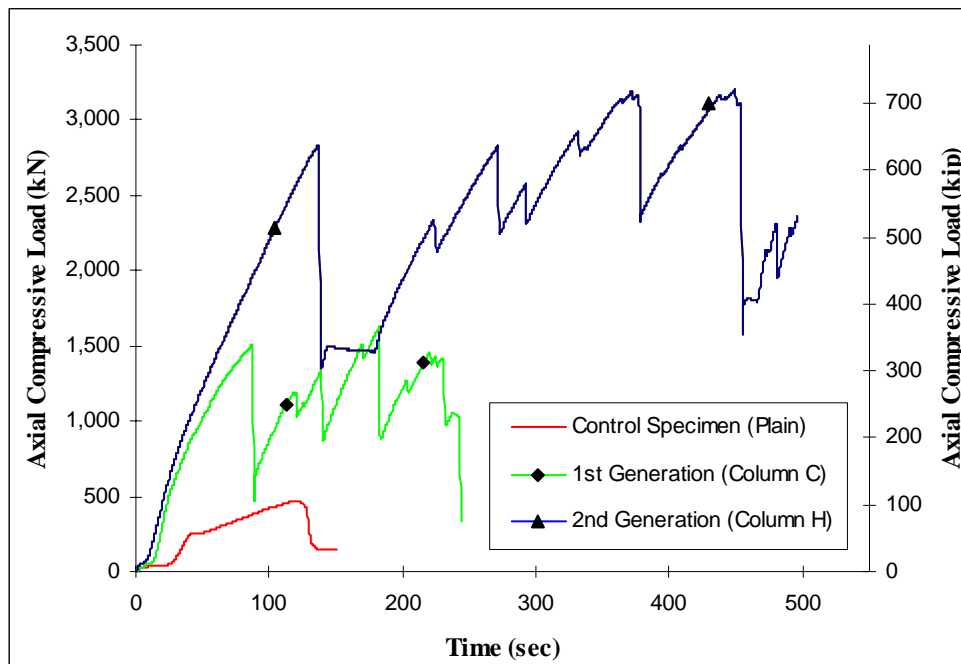


FIGURE 33 LOAD-TIME HISTORY SHOWING LOAD TRANSFER DUE TO CIRC FAILURE

Figure 33 compares a 2nd generation column with the strongest 1st generation column (Column C) and a control specimen. This figure shows the large increase in strength and significant drop in load as each end circ failed. The next figure shows how the stress in these 2nd generation columns (Column H) is transferred as these circs failed (see Figure 34).

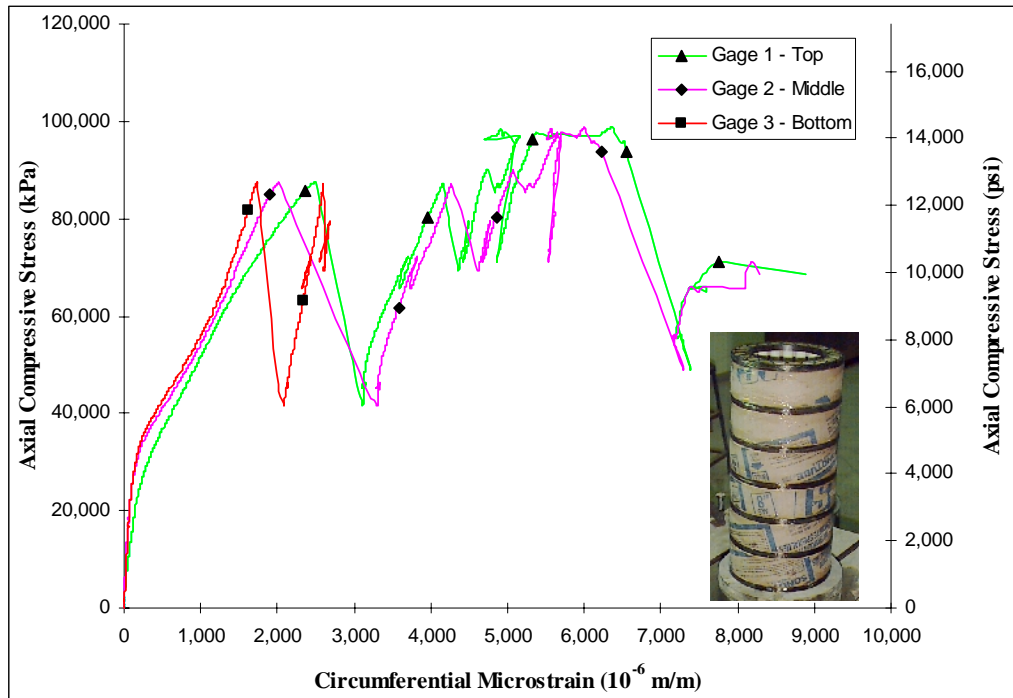


FIGURE 34 AXIAL STRESS VERSUS CIRCUMFERENTIAL STRAIN FOR 2ND GENERATION COLUMN

In Figure 33, gage 1 is labeled the “Top”, but is actually located on the 3rd circ down from the top of the column, while the middle circ is the 4th down (Middle of seven circs) and the 3rd gage is located on the circ just below the “Middle” gage. During the test, the first circ failed at 3.1 MN (700 kip) which correlates with the first drop in stress at 85 MPa (12 ksi). The next circ failed at 3.2 MN (720 kip) which correlates with the second drop in stress at 97 MPa (14 ksi). Gage 1 was closest to the end failure and consequently shows the highest strain value during the first circ failure while gage 3 shows the lowest strain value because it is the farthest from the failure. This plot shows how the strength of the circumferential reinforcement controls the ultimate strength of the column in compression.

These axial compression tests on the second generation columns also confirm that the number of longitudinal reinforcement members in the composite grid structure correlates directly with the initial slope of the stress-strain curve. Second generation columns G, H and I all had 21 longis, and the initial slope of each column is almost identical (see Figure 35).

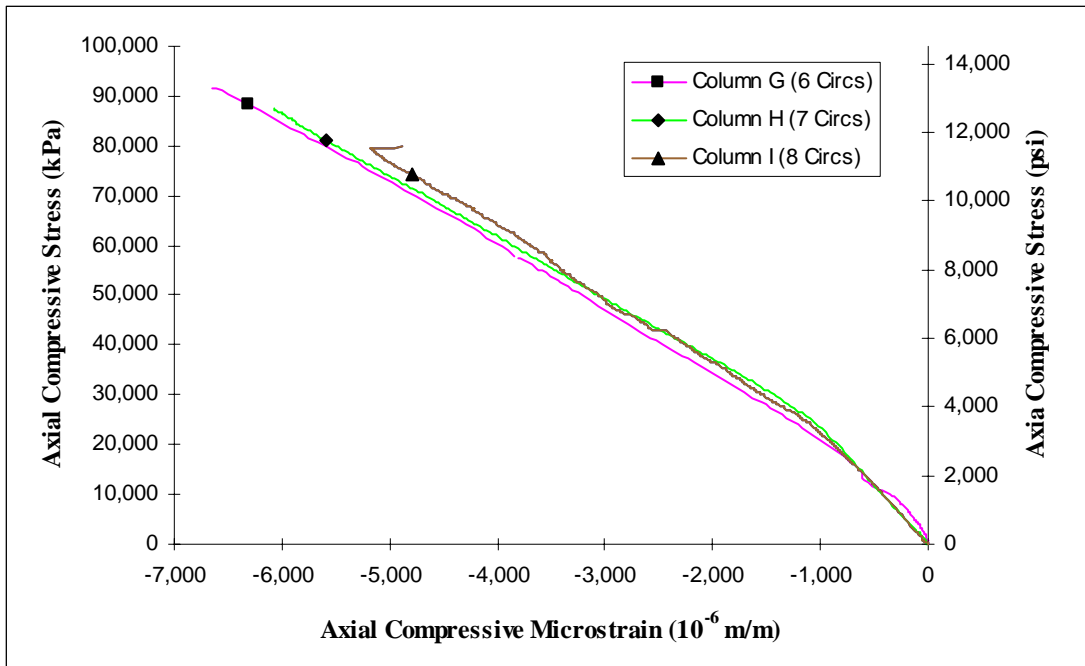


FIGURE 35 AXIAL COMPRESSIVE STRESS VERSUS STRAIN IN 2ND GEN. LONGITUDINAL REINFORCEMENT

7.5 COMPARISON OF FIRST AND SECOND GENERATION COLUMNS

A comparison was made between the different generations of circs by plotting the ultimate load and the number of longitudinal reinforcement bars (see Figure 36). The first and second generation columns suggest that the primary factor determining the failure of composite grid reinforced concrete columns is the strength of the circumferential reinforcement with a secondary factor being the longitudinal reinforcement. The fiberglass longis contain the concrete with their bending properties while the carbon circs contain the concrete with their tensile properties. This synergistic containment of the concrete prevents the column from expanding radially, delaying the primary mode of failure. A comparison between the first two generations of grid structures was also made by plotting the ultimate load and number of circumferential reinforcement (see Figure 37). Again, the results show that the strength of circumferential reinforcement controls the axial strength of the columns, while the spacing and percentage of circumferential containment only partially contributes to the strength. These observations were used to design the 3rd generation columns.

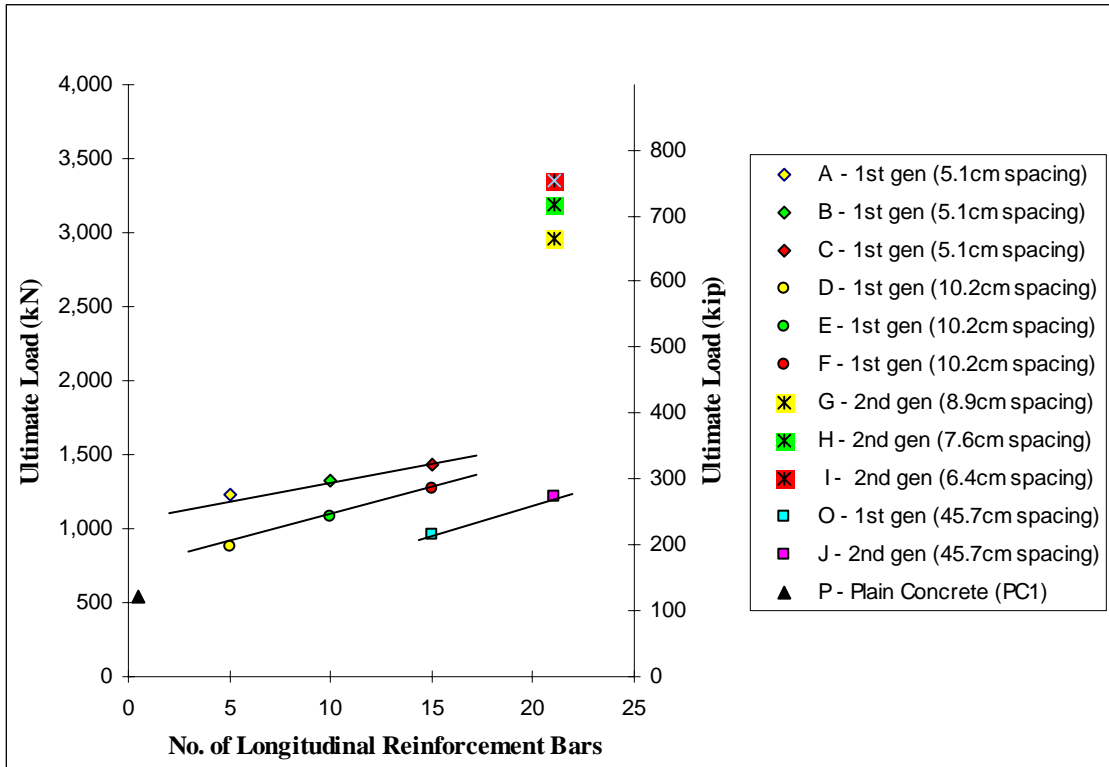


FIGURE 36 INFLUENCE OF LONGITUDINAL REINFORCEMENT ON 1ST AND 2ND GENERATION COLUMNS

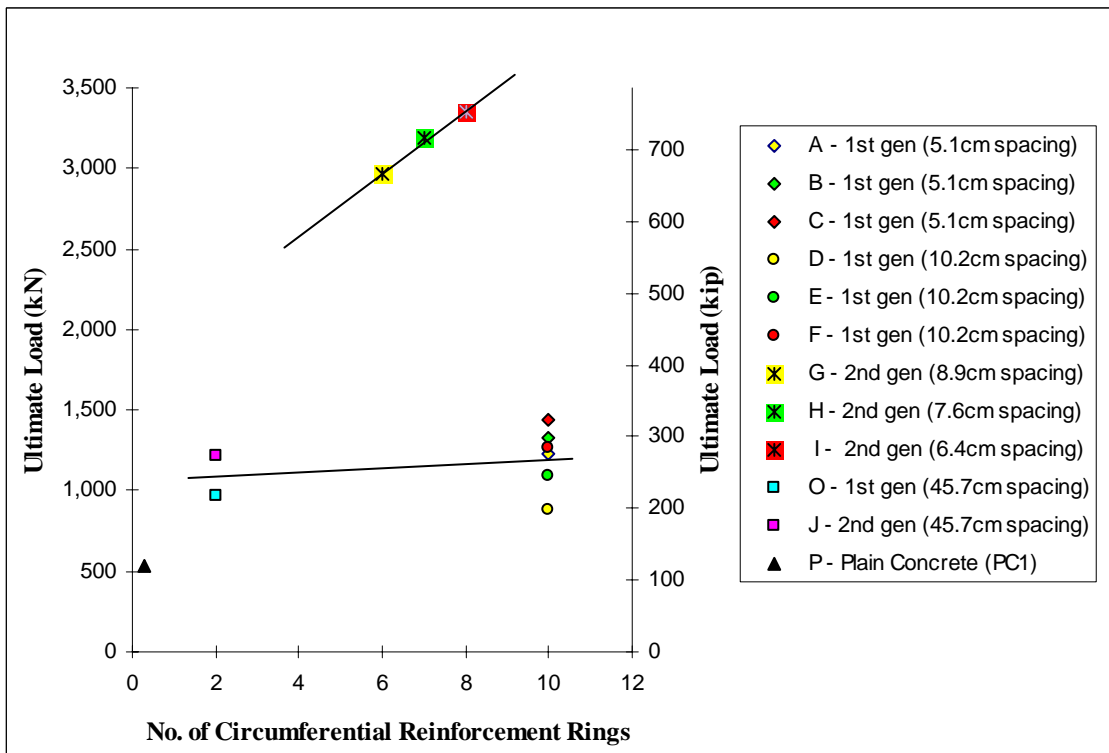


FIGURE 37 INFLUENCE OF CIRCUMFERENTIAL REINFORCEMENT ON 1ST AND 2ND GENERATION COLUMNS

7.6 THIRD GENERATION COLUMNS

The third generation columns failed in a similar manner as the 1st and 2nd generation columns; however a much higher compressive load was reached by focusing on principles learned from previous testing. Steel endcaps were used in order to prevent end failure and focus on containment. Two columns of the same geometry were constructed; one was tested with steel endcaps and one without (see Figure 38 and Figure 39).

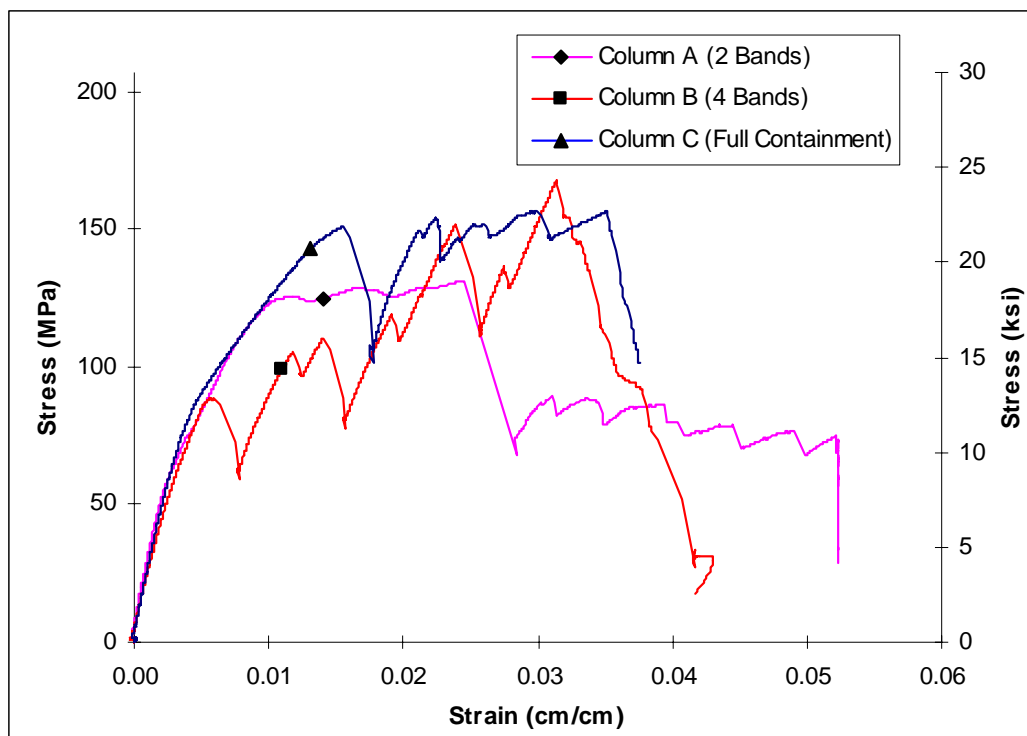


FIGURE 38 STRESS VERSUS STRAIN FOR 3RD GENERATION WITHOUT STEEL ENDCAPS

Even without the steel endcaps these third generation columns reached ultimate loads around 3.6 MN (800 kip) or 150 Mpa (22 ksi). This is five times the strength of the control specimens and almost three times the strength of the 1st generation grid structures. Column C with full Containment showed the highest strength at 3,665 kN (824 kip) while Column A with only partial containment at the ends of the column (40% containment) failed at 3,196 kN (720 kip). Column B with 80% containment failed at 3,523 kN (792 kip). There was not a large difference in ultimate strength between these columns; however Figure 39 shows the effect of mitigating end failure.

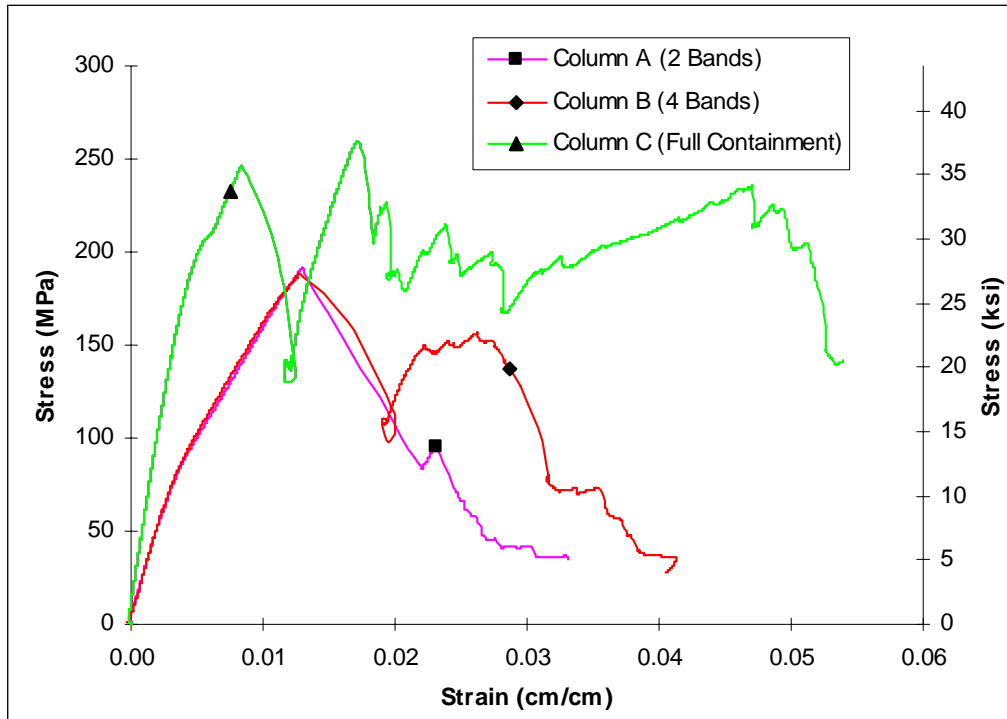


FIGURE 39 STRESS VERSUS STRAIN FOR 3RD GENERATION WITH STEEL ENDCAPS

Column C with full containment showed an ultimate strength of 4,750 kN (1,070 kip), while Column B with 80% containment reached 4,662 kN (1,048 kip) and Column A at 40% containment with 4,560 kN (1,026 kip). An important feature of this graph is the increase in toughness that is shown with the increase in containment. Table 7 summarizes these results.

TABLE 7 COMPARISON OF 3RD GENERATION COLUMNS

Column ID	Containment Type	Steel Endcaps	Ultimate Strength [kN (kip)]	Ultimate Pressure [MPa (ksi)]	Toughness (u_f) [kPa (psi)]
CS	Control - Plain	No	1,090 (245)	59.74 (8.67)	128 (18.6)
A1	2 Endwraps	No	3,196 (719)	131.83 (19.12)	2,950 (428)
A2	2 Endwraps	Yes	4,660 (1048)	192.16 (27.87)	1,730 (251)
B1	4 Wraps	Yes	4,562 (1026)	188.14 (27.29)	4,190 (608)
B2	4 Wraps	No	4,068 (915)	167.76 (24.33)	3,850 (558)
C1	Full	Yes	2,856 (642)	117.77 (17.08)	8,430 (1,220)
C2	Full	No	3,665 (824)	151.16 (21.92)	4,500 (653)
C3	Full	Yes	4,760 (1070)	196.29 (28.47)	8,190 (1,190)
D1	PVC - 1 lam	No	1,068 (240)	58.52 (8.49)	1,260 (183)
D2	PVC - 1 lam	No	1,174 (264)	64.38 (9.34)	1,590 (231)
Avg of A,B, & C W/out Steel Endcaps			3,643 (819)	150.25 (21.79)	- -
Avg of A,B, & C W/ Steel Endcaps			4,026 (905)	166.03 (21.08)	- -

CHAPTER 8

FAILURE MODES

8.1 TYPICAL SHEAR FAILURE

Plain concrete columns typically fail due to shear which is evident in a 45° to 60° angle crack after failure. Reinforced concrete columns can be subjected to shear plus axial tensile or compressive forces due to such causes as gravity load effects in inclined members, stresses resulting from restrained shrinkage, wind and seismic forces [MacGregor, 1997]. Figure 40 shows a tied column that failed in shear during the 1971 San Fernando, California Earthquake.



FIGURE 40 PHOTOGRAPH OF SHEAR FAILURE IN REINFORCED COLUMN

8.2 1ST GENERATION COLUMNS

For the 1st generation columns, failure generally initiated at one end of the column. When the preliminary tests were performed, the concrete between the circumferential reinforcement could be seen “bulging” due to lack of containment (see left photo in Figure 41).



FIGURE 41 PRELIMINARY TEST AND END FAILURE FOR CONFIGURATION WITH 6 CIRCS, 5 LONGIS

The concrete crumbled locally, the end circ slid down the longis, and the ends of the pultruded longis exhibited brooming. Soon after this, one of the end circs would fail which would further broom out the longis and increase the area over which the load was applied. Tests were also performed on this same grid structure at Hong Kong University where these columns failed in a similar manner at one end of the column (see the right photograph in Figure 41).

The first generation columns showed a dramatic failure due to the outer concrete layer which spalled off during failure. As the circs expanded the outer concrete separated from the 7 inch diameter core of concrete contained by the advanced composite grid structure. For the 1st generation columns this was when the load reached approximately 1.3 MN (300 kips). A slight drop in load indicated the initiation of cracking, followed by separation of the outer layer of concrete in the form of high velocity projectiles. After this initial failure the load continued to climbed steadily until a sudden failure initiated at one end of the column (see Figure 42).

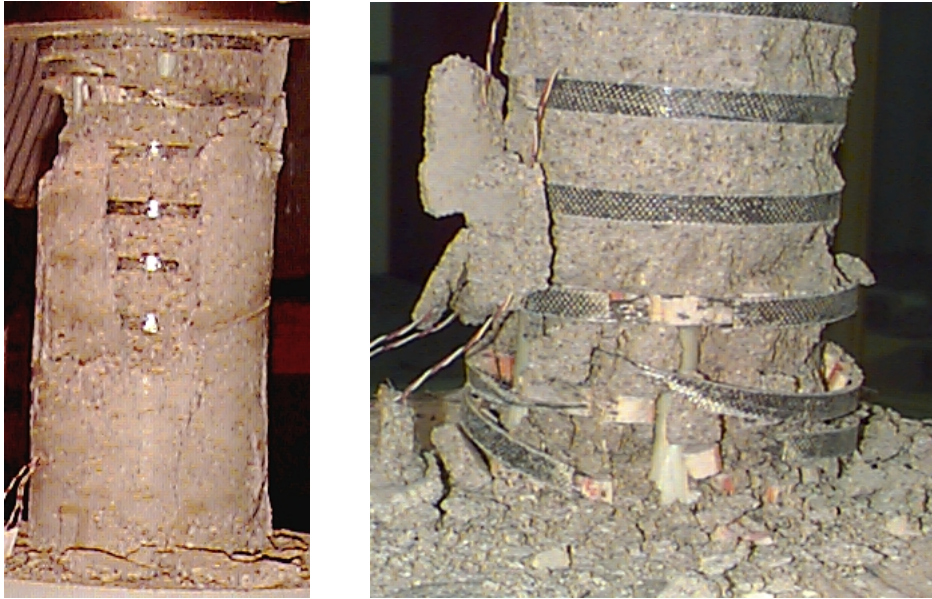


FIGURE 42 PHOTOGRAPHS OF COLUMN A IN AXIAL COMPRESSION, SHOWING SPALLING & END FAILURE

Column B showed a similar failure with initial spalling of the outer concrete and then a dramatic end failure which initiated at one end of the column and resulted in brooming of the longis as the individual end circs failed (see Figure 43).



FIGURE 43 PHOTOGRAPHS OF COLUMN B IN AXIAL COMPRESSION, SHOWING BROOMING OF THE LONGIS

Column C did not display as much brooming during failure, most likely due to the increased number of longis (15) which helped to contain the concrete. Failure initiated at the bottom of the column where three circs failed before the load dropped significantly. The outer concrete began to crack at 1.11 MN (250 kip) but the first failure did not occur until the load reached 1.55 MN (350 kip). After this bottom end circ failed the load dropped to 0.67 MN (150 kip) but began to immediately rise again (see Figure 28 in Chapter 7). The next failure occurred at a load of 1.3 MN (300 kip) when the second circ failed. Again, the load began to rise, this time to 1.65 MN (360 kip) – an ultimate load greater than the first initial failure! This is when the 3rd circ failed and the column could no longer sustain an increase in load (see Figure 44).

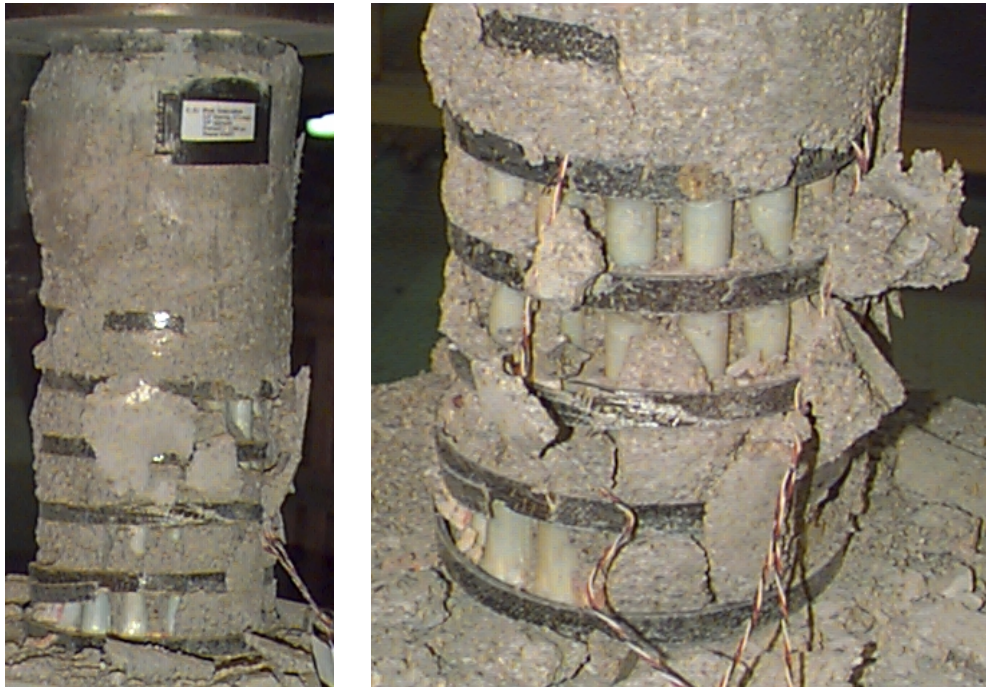


FIGURE 44 PHOTOGRAPHS OF COLUMN C IN AXIAL COMPRESSION, SHOWING FAILURE OF CIRC

Although the number of circs was kept constant (10) for the majority of the first generation columns, a grid structure was constructed using only two circs in order to demonstrate the effectiveness of the carbon fiber circs in not only containing the concrete but preventing buckling of the longis. Column O was created using a fully packed number of longis (15) with one circ at each end. While Columns A – F had a containment area of approximately 30% with the use of 10 circs, Column O had an effective containment area of only 6%. This test was important because it showed how weak the 1st generation circs were in comparison to the 2nd generation circs .

The axial compression test of Column O showed that the first mode of failure for these columns (after the outer concrete spalled off) was an end failure (see Figure 45). If these first generation circs had been strong enough to resist this end failure, buckling of the longis would have been the next failure mode as shown in the second generation Column J.



FIGURE 45 PHOTOGRAPHS OF COLUMN O, SHOWING END CIRC FAILURE BEFORE BUCKLING OF LONGIS

Columns D, E, and F used the same variation of longis as Columns A, B, and C; however, the doubling of circs showed some surprising results (see Figure 46).

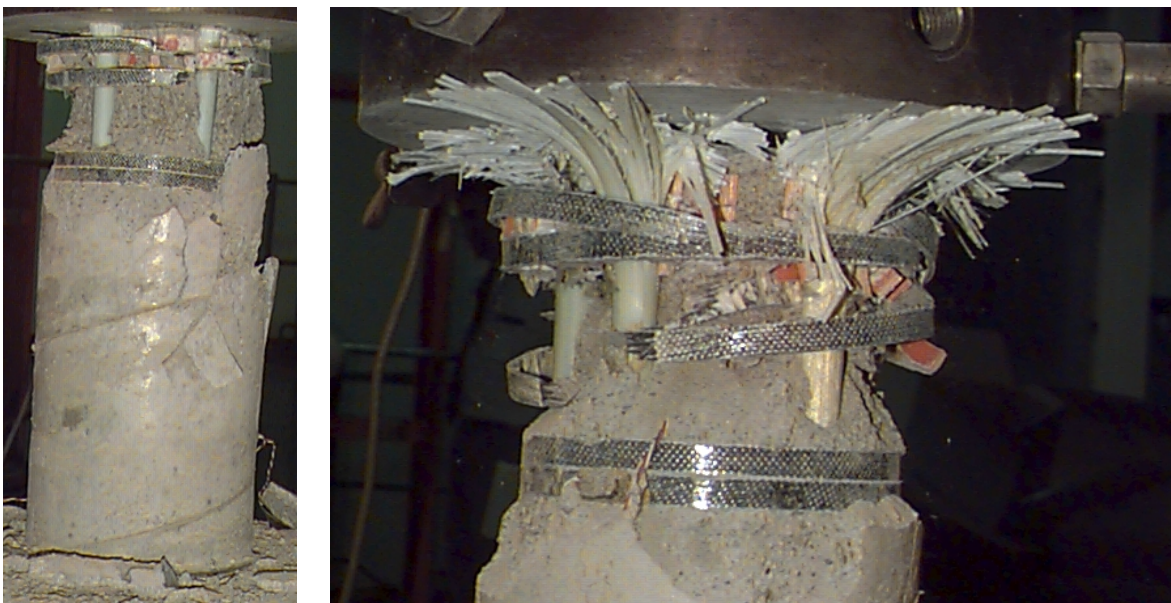


FIGURE 46 PHOTOGRAPHS OF COLUMN D IN AXIAL COMPRESSION, END FAILURE WITH DOUBLED CIRCS SHOWN

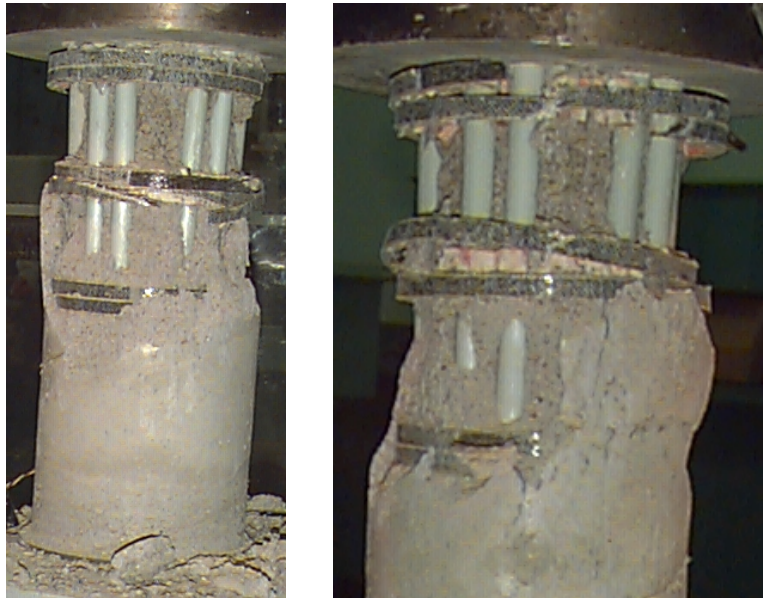


FIGURE 47 PHOTOGRAPHS OF COLUMN D IN AXIAL COMPRESSION, DOUBLE CIRC FAILURE

When the circs were not spaced throughout the column, the middle of each column was not allowed to expand radially which increased the stress at the end of each column and reduced the ultimate load (see Figure 47). Column E is an example of this failure where photographs show a failure at both ends of the column without first spalling the outer concrete (see Figure 48).

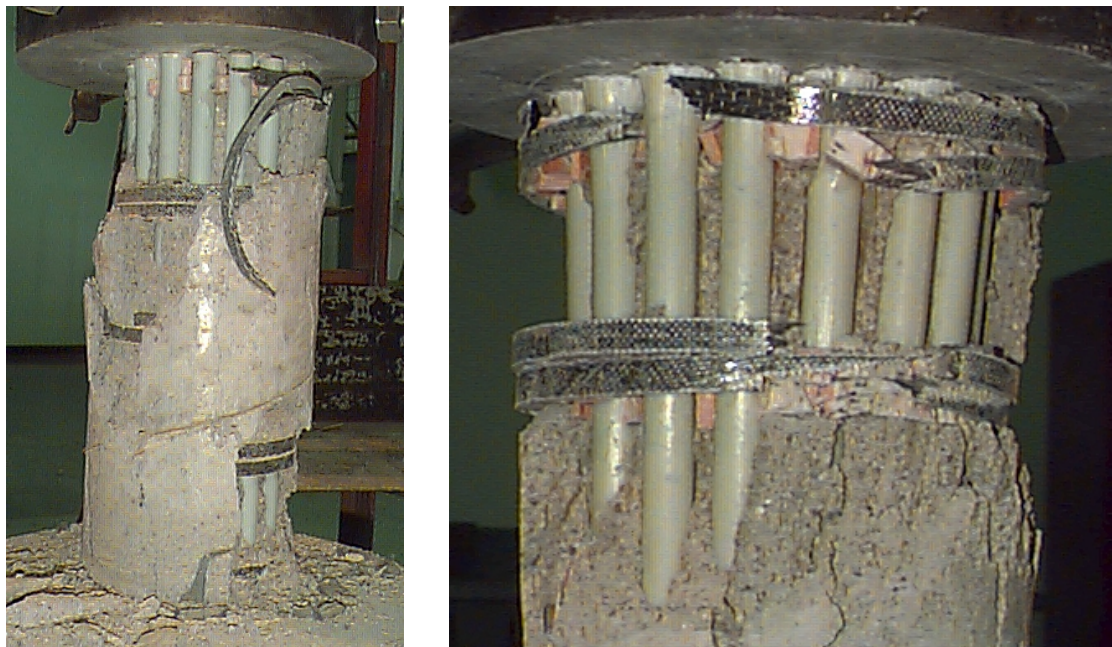


FIGURE 48 PHOTOGRAPHS OF COLUMN E IN AXIAL COMPRESSION, END FAILURE AT BOTH ENDS OF THE COLUMN

8.3 2ND GENERATION COLUMNS

The 2nd generation columns showed a similar failure mode to the 1st generation column; however, because of the larger diameter of these circs more concrete was contained in the core of the composite grid structure and less concrete was spalled off at initial failure (see Figure 49).



FIGURE 49 PHOTOGRAPHS OF COLUMN G IN AXIAL COMPRESSION, END FAILURE SHOWN

Due to the high quality of the carbon fiber used in these 2nd generation circs, the columns were not as dramatic in nature during failure as the 1st generation columns. The failure initiated at one end of the column, but the concrete suffered little deformation due to the containment of circs and number of longis used in the configuration.

Column H with 7 circs and 21 longis is a good example of the 2nd generation columns' ability to repeatedly release stress through circ failures without a significant drop in load. The initial cracking of the outer concrete began at 1.33 MN (300 kip) yet the first failure did not occur until compression load built up to 3.90 MN (660 kip)! Once this first end circ failed the load dropped to 1.42 MN (320 kip) and built back up 3.11 MN (700 kip) before the second failure. The load then dropped to only 2.27 MN (510 kip) before failing the third circ at 3.11 MN (700 kip) once again. The increased ductility of these columns is amazing considering the amount of load sustained without an abrupt failure as shown in steel reinforced columns. These columns did exhibit some brooming but nothing like that shown in 1st generation columns (see Figure 50).



FIGURE 50 PHOTOGRAPHS OF COLUMN H IN AXIAL COMPRESSION, BROOMING OF LONGIS SHOWN

Column I showed similar results to the other 2nd generation columns, with little brooming of the longis shown after the initial failure of the end circ (see Figure 51).

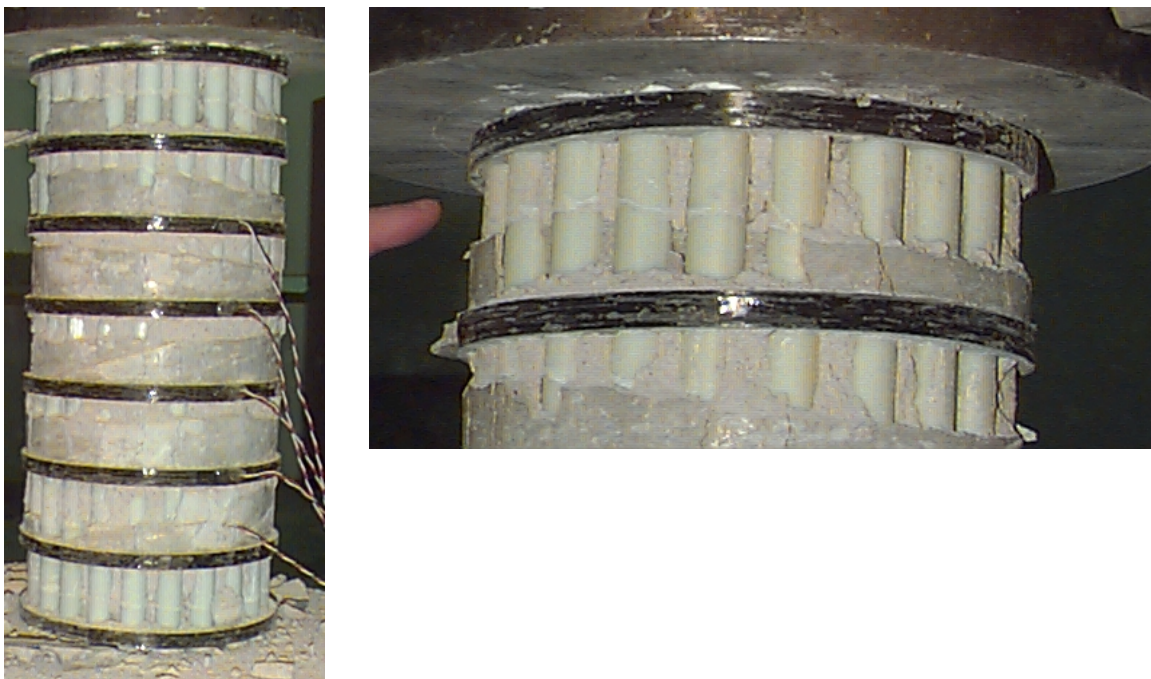


FIGURE 51 PHOTOGRAPHS OF COLUMN I IN AXIAL COMPRESSION, END FAILURE WITH END CIRC STILL IN TACT

Similar to Column O in the first generation of columns, a second generation column was created using a fully packed grid of longis (21) but only two end circs. These test results confirmed that a stronger circ could resist end failure and force the mode of failure to buckling of the longis. Here the 2nd generation circs show that they are effective in both containing the concrete but also preventing the buckling of the longis (see Figure 52).



FIGURE 52 PHOTOGRAPH OF COLUMN J IN AXIAL COMPRESSION, BUCKLING OF THE LONGS

8.4 3RD GENERATION COLUMNS

As discussed in chapter 3, this generation of columns was constructed using a technique for strengthening of existing columns; however, the failure modes were fairly similar and the increase in load was just as high as the 2nd generation columns. Three main types of failures were seen depending upon the configuration of composite reinforcement and the use of steel endcaps. The first is failure of the 10.2 cm (4.0 in.) fiberglass wraps (similar to the failure of the 1st and 2nd generation circs), the second is buckling of the longis, and the third is rupture of the entire column, where the fiberglass wraps and full containment core shear at the same time.

The use of steel endcaps had a significant effect upon the type of failure seen in axial compression. Column A showed a buckling of the longis with the use of steel endcaps and a rupture of the column when this end effect was not controlled (see Figure 53).

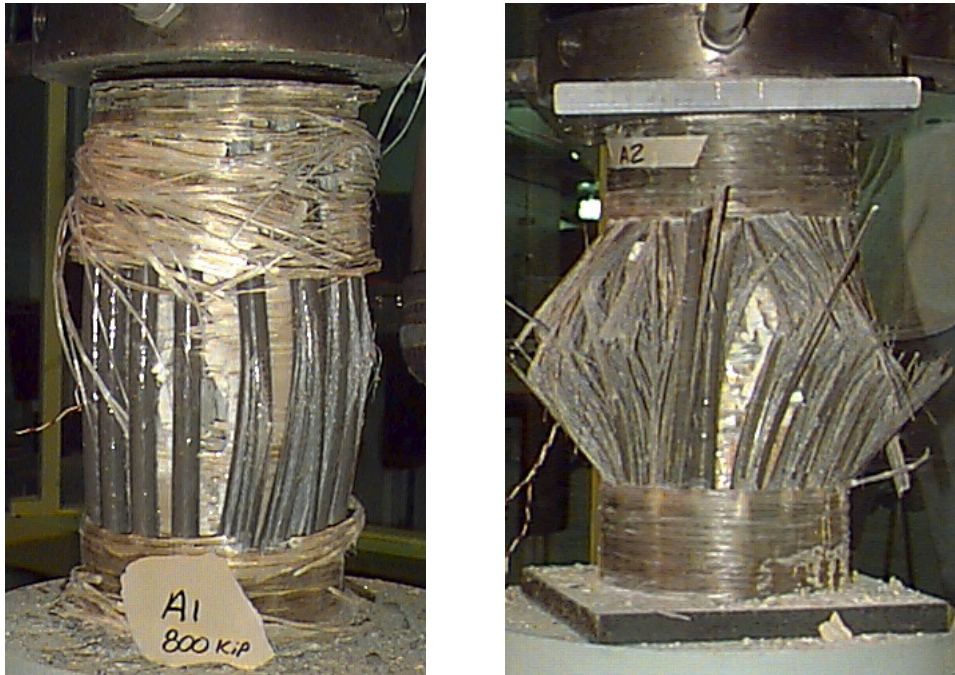


FIGURE 53 COLUMN A IN AXIAL COMPRESSION, SHOWING RUPTURE & BUCKLING



FIGURE 54 COLUMN B IN AXIAL COMPRESSION, SHOWING FAILURE OF 4" END WRAPS

Column B shows a failure of the 10.2 cm (4.0 in.) fiberglass endwraps. Once these wraps failed in tension due to the radial expansion of the columns, containment of the concrete was lost and the core of the concrete as well as the inner fiberglass windings ruptured (see Figure 54). Column C which used full containment along the outside of the column also showed failure of the hoop wound fiberglass windings. Once this containment failed the inner core of concrete again ruptured in shear (see Figure 55).

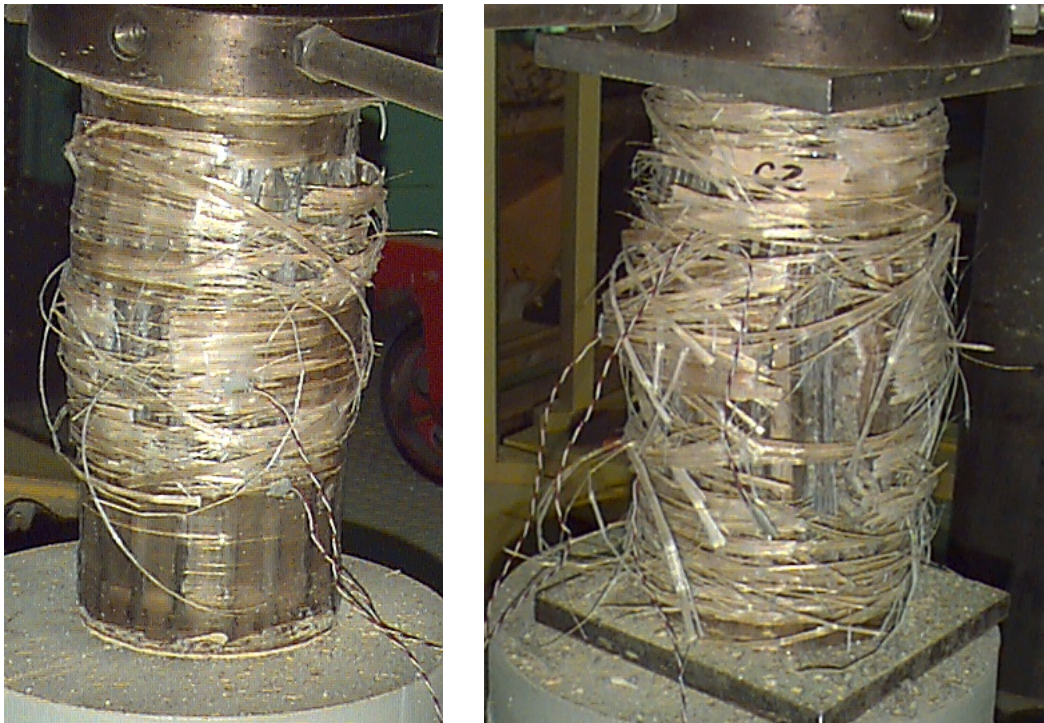


FIGURE 55 COLUMN C IN AXIAL COMPRESSION, FAILURE OF CONTAINMENT & RUPTURE OF CORE

Third generation Columns A, B, and C showed exciting results because they were reaching loads of 190 MPa (27.3 ksi) with the steel endplates and 140 MPa (20.3 ksi) without the endplates. As discussed in chapter 3, the core of these 3rd generation columns (Column D) was also tested in order to demonstrate the importance of the longitudinal reinforcement and outer containment of fiberglass windings. Without the synergistic effect of the longis, these columns with only the inner full containment failed at relatively low values, 60.7 MPa (8.8 ksi). Compared with the control specimens (5 ksi mix design), these columns showed an increase in compressive strength with containment; however, these tests also show that the use of longitudinal reinforcement with additional outer reinforcement is vital to the strength of these 3rd generation columns. Two of these “core” columns were tested and demonstrated two types of failure (see Figure 56).

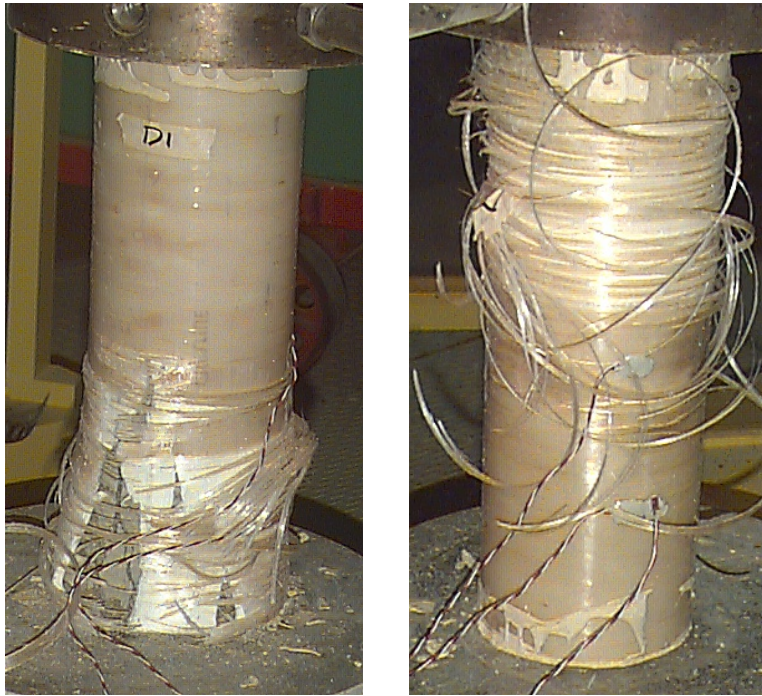


FIGURE 56 PHOTOGRAPHS OF COLUMN D IN AXIAL COMPRESSION

This “core” of the 3rd generation columns showed an end failure in the first test where the fiberglass hoop windings failed in tension and the PVC pipe and concrete core then ruptured. The second test shows a complete failure of the fiberglass containment beginning at the top of the column and propagating downward.

CHAPTER 9

DISCUSSION OF RESULTS

9.1 FAILURE MODES

For these advanced composite grid structures, the longitudinal rods resist flexure while the carbon fiber rings or partial fiberglass wraps contain the concrete under axial compression. The containment of the concrete prevents the column from expanding radially, delaying the primary mode of failure. This shear failure (evident in a 45° to 60° angle crack after failure) was resisted by these advanced composite grid structures offering proof for the conceptual design being tested in this research. The 1st and 2nd generation columns suggest that the primary factor determining failure of composite grid reinforced concrete columns is the strength of the circumferential reinforcement with a secondary factor being the longitudinal reinforcement. A full containment jacket made of high quality windings should, therefore, yield the highest strength. This theory was tested and proven with the 3rd generation columns.

This shift away from the primary mode of failure in plain concrete columns led to much higher ductility and axial compressive strength; however, three different modes of failures resulted. These three modes of failure which differed in degree and combination are: 1) end failure due to local crumbling of the concrete, 2) circum failure due to radial expansion of the column which exceeded the tensile strength of the hoop windings, and 3) buckling of the longis due to lack of circumferential containment. The first generation columns displayed these first two failure modes. The concrete crumbled locally, the end circum slid down the longis and the ends of the pultruded longis exhibited brooming. This failure was magnified by the relatively weak circum which would eventually fail, sending the crumbling cover concrete flying away from the column, and allowing further bending and brooming of the longis. The second generation

columns failed in a similar manner with further bending and brooming of the longis resulting in successive circ failures. The third generation column with steel endplates were able to resist these end effects and consequently failure modes two or three resulted depending upon the amount of circumferential containment used in the grid configuration. Either radial expansion of the column would eventually exceed the tensile strength of the fiberglass hoop winding resulting in rupture of the containment (see Figure 55) or else the longis would buckle due to lack of circumferential containment (see Figure 53).

9.2 STRESS-STRAIN BEHAVIOR

The stress-strain behavior for the circumferential reinforcement of the columns was affected by the number of longis resisting flexure and especially the number of circs used for partial containment. The stress-strain diagram for the 1st and 2nd generation columns was interesting in this respect. As the first circ failed, the stress dropped dramatically and the strain increased for the remaining circs in the columns. Typically, one would expect the strain to decrease as the stress dropped. This occurrence is likely due to the stroke control of the compression machine, coupled with the radial expansion of the columns. In between failures of end circs, the stress-strain relationship is essentially linear, with the original axial stiffness.

The initial slope of the axial stress-strain curves for the longitudinal reinforcement was only slightly affected by the number of longis used in the grid configuration. Yet, the circumferential stress-strain curve for the circs was very different with an increase in the number of longis. This suggests that an increase of longitudinal reinforcement does not contribute so much to axial stiffness as it does to helping the circ contain the concrete for a dramatic increase in axial compressive strength.

9.3 LOAD TRANSFER EFFECTS

The compressive strength of concrete is significantly increased with even minimal reinforcement. Likewise, tests performed on grids without concrete exhibited relatively low capacity. The ultimate compressive strength of grid reinforced concrete suggests that the load is

being carried synergistically between both components. The stress-strain diagrams indicate that the concrete takes most of the load up to its “yield” point, after which the composite grid takes over. Without support the longis would buckle at relatively small compression loads. The circs and concrete brace the longis, while the circs and longis confine the concrete. The concrete layer outside of the composite grid structure is not an integral part of the load transfer between the concrete and composite. At the load where plain concrete columns fail, the reinforced columns exhibited separation of the external concrete from the grid structure.

The axial compressive strength of these partially contained columns is highly dependent upon the tensile strength of the circumferential reinforcement. The 2nd generation columns were far superior to the 1st generation columns, and the 3rd generation columns (which used fiberglass windings instead of carbon fiber) were just as strong in axial compression as the 2nd generation columns. These 3rd generation columns also have the ability to be applied to existing columns for rehabilitation and seismic retrofit. This high strength from the 2nd and 3rd generation columns was mostly due to the higher quality windings, rather than the additional number of longis. These columns were averaging an ultimate compression strength increase of five to six times that of the plain concrete specimens. Although the different generation of columns failed at different loads, the load transfer behavior between the composite grid structure and inner concrete was very similar and gives support to the viability of this design concept.

9.4 OPTIMIZATION OF GEOMETRIC CONFIGURATION

Columns A through F consisted of 10 1st generation circs spaced at different intervals with 5 to 15 longis. Although these grids exhibited two to three times the strength of plain concrete, doubling the number of longis (from 5 to 10) only modestly increased the ultimate compressive strength (8% and 24% for narrow and wide spacing, respectively). Increasing the number of longis to 15 yielded an additional strength increase of 4% for narrow (5.1 cm) and 17% for wide (10.2 cm) spacing yielding a combined increase of 13% and 45%, respectively, for tripling the number of longis. Since the fiberglass is stiffer than the concrete, the stiffness also increased slightly with the number of longis. The axial compression tests on the 2nd generation columns also confirm that the number of longis affects the initial slope of the stress-strain curve. Columns G, H, and I each had 21 longis, and the initial slope of each column is almost identical.

These tests also proved that doubling the density of the circs by spacing them closer together was considerably more effective than doubling the density of the circs by spacing two circs at each location. This increase in strength with smaller spacing intervals suggests that total containment of the column should yield the highest ultimate compressive strength. The test results on the first and second generation columns suggested that the more surface area confined, the greater the axial compressive strength of the columns. This was confirmed by comparing the ultimate strength of the 2nd generation columns. Although these columns had over twice the compressive strength of the 1st generation columns and over five times the strength of plain concrete, the strongest column had the largest number of circs. Thus, optimization of these advanced composite grid structures for concrete columns points to either full containment or partial containment using high strength circumferential reinforcement spaced at small intervals. More circumferential reinforcement increases the ultimate strength. The cost-to-benefit ratio, however, may prove partial containment using high strength circumferential reinforcement to be more cost effective.

9.5 PARTIAL VS. FULL CONTAINMENT

Because the initial focus of this research was to optimize the geometric configuration of circs and longis in composite grid structures, priority was given to keeping the number of circs the same and varying the number of longis. Once it was discovered that the quality and amount of containment was the major contributor to overall compressive strength, then priority was given to the percentage of area contained by the advanced composite grid structure. This was the real focus of the 3rd generation columns. The test matrix for this generation of columns allowed for a comparison between full and partial containment using the same number of longis and type of material used while varying the amount of circumferential containment. For this reason, overall comparisons between the three different generations were based on the amount of circumferential containment by surface area. This allowed for a comparison between each of the different generations of columns (see Table 8).

TABLE 8 COMPARISON BETWEEN 1ST, 2ND, AND 3RD GENERATION COLUMNS BY CONTAINED AREA

Column ID	Number of Circs	Spacing [cm (in)]	Contained Area	Number of Longis	Aggregate Size [cm (in)]	Ultimate Load [kN (kip)]	Average [kN (kip)]
1st Generation							
A.1	10	5.1 (2.0)	25%	5	6.4 (0.25)	1,191 (268)	
A.2	10	5.1 (2.0)		5	6.4 (0.25)	1,260 (283)	1,226 (276)
B.1	10	5.1 (2.0)	25%	10	6.4 (0.25)	1,274 (287)	
B.2	10	5.1 (2.0)		10	6.4 (0.25)	1,381 (310)	1,328 (299)
C.1	10	5.1 (2.0)	25%	15	6.4 (0.25)	1,253 (282)	
C.2	10	5.1 (2.0)		15	6.4 (0.25)	1,510 (340)	1,382 (311)
D.1	10	10.2 (4.0)	25%	5	6.4 (0.25)	980 (220)	
D.2	10	10.2 (4.0)		5	6.4 (0.25)	771 (173)	876 (197)
E.1	10	10.2 (4.0)	25%	10	6.4 (0.25)	1,086 (244)	
E.2	10	10.2 (4.0)		10	6.4 (0.25)	1,086 (244)	1,086 (244)
F.1	10	10.2 (4.0)	25%	15	6.4 (0.25)	1,374 (309)	
F.2	10	10.2 (4.0)		15	6.4 (0.25)	1,157 (260)	1,266 (284)
O	2	45.7 (18.0)	5%	15	6.4 (0.25)	966 (217)	966 (217)
K	-	-	-	-	6.4 (0.25)	468 (105)	468 (105)
2nd Generation							
G	6	6.4 (2.5)	15%	21	9.5 (0.38)	2,965 (667)	2,965 (667)
H	7	7.6 (3.0)	18%	21	9.5 (0.38)	3,190 (717)	3,190 (717)
I	8	8.9 (3.5)	20%	21	9.5 (0.38)	3,346 (752)	3,346 (752)
J	2	45.7 (18.0)	5%	21	9.5 (0.38)	1,220 (274)	1,220 (274)
M	-	-	-	-	9.5 (0.38)	571 (128)	571 (128)
3rd Generation							
A.1	2 Wraps	40.6 (18.0)	40%	18	9.5 (0.38)	3,196 (719)	3,196 (719)
A.2	2 Wraps*	40.6 (18.0)	40%	18	9.5 (0.38)	4,564 (1026)	4,564 (1026)
B.1	4 Wraps*	13.5 (5.3)	80%	18	9.5 (0.38)	4,662 (1048)	4,662 (1048)
B.2	4 Wraps	13.5 (5.3)	80%	18	9.5 (0.38)	3,523 (792)	3,523 (792)
C.1	Full*	-	100%	18	9.5 (0.38)	2,856 (642)	2,856 (642)
C.2	Full	-	100%	18	9.5 (0.38)	3,665 (824)	3,665 (824)
C.3	Full*	-	100%	18	9.5 (0.38)	4,760 (1070)	4,760 (1070)
D.1	Full	-	100%	18	9.5 (0.38)	1,174 (264)	1,174 (264)
C.S.	-	-	-	-	9.5 (0.38)	1,090 (245)	1,090 (245)

* STEEL ENDCAPS USED IN AXIAL COMPRESSION TEST

As explained earlier, the initial focus of the first generation columns was placement of the circs and the number of longis used in the grid configuration. Consequently, only a few data points were available for comparing the amount of circumferential containment by area and ultimate compressive load. A total of 10 circs used in this column generation resulted in approximately 25% circumferential containment of the total area of the column. Column O which used only two circs made up only 5% circumferential containment. Despite the few data points available for this study, an interesting trend line was developed using Columns C, F and O (see Figure 57).

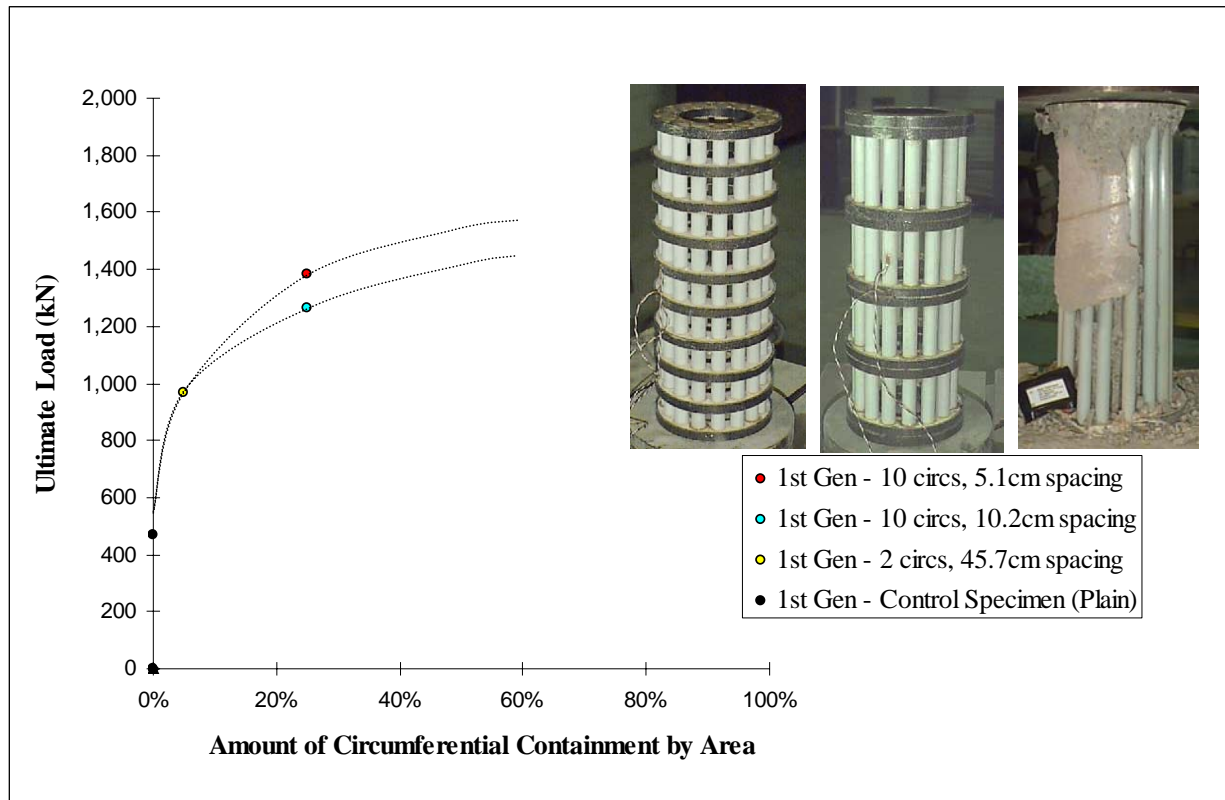


FIGURE 57 COMPARISON OF 1ST GENERATION COLUMNS IN AXIAL COMPRESSION BY AMOUNT OF CONTAINMENT

A comparison between area of containment and ultimate load for the 2nd generation columns was also made. More data was available because of the number of circs that were varied in the grid configurations. The number of longis were kept constant at 21 and the percentage of containment varied 5, 15, 18, and 20 according to the use of 2, 6, 7 and 8 circs respectively. The trend line for this data showed a steady rise in ultimate load as the amount of circumferential containment was increased; however, it was unclear what the ultimate load would be at a much higher percentage of containment (see Figure 58). This same comparison for the 3rd generation of grid structures was also plotted and showed some interesting results. Column A, B and C varied in 40, 80 and 100 percent containment respectively. Data was plotted for each column with and without steel endcaps. The trend lines are similar for both of these curves; yet, there is a gap of approximately 1500 kN (335 kip) due to the increase in strength with the use of endcaps. Similar to the 2nd generation columns there is a part of the trend line that is unclear; however, in the case of the 3rd generation columns it is the first part of the curve where less than 40% containment is used (see Figure 59).

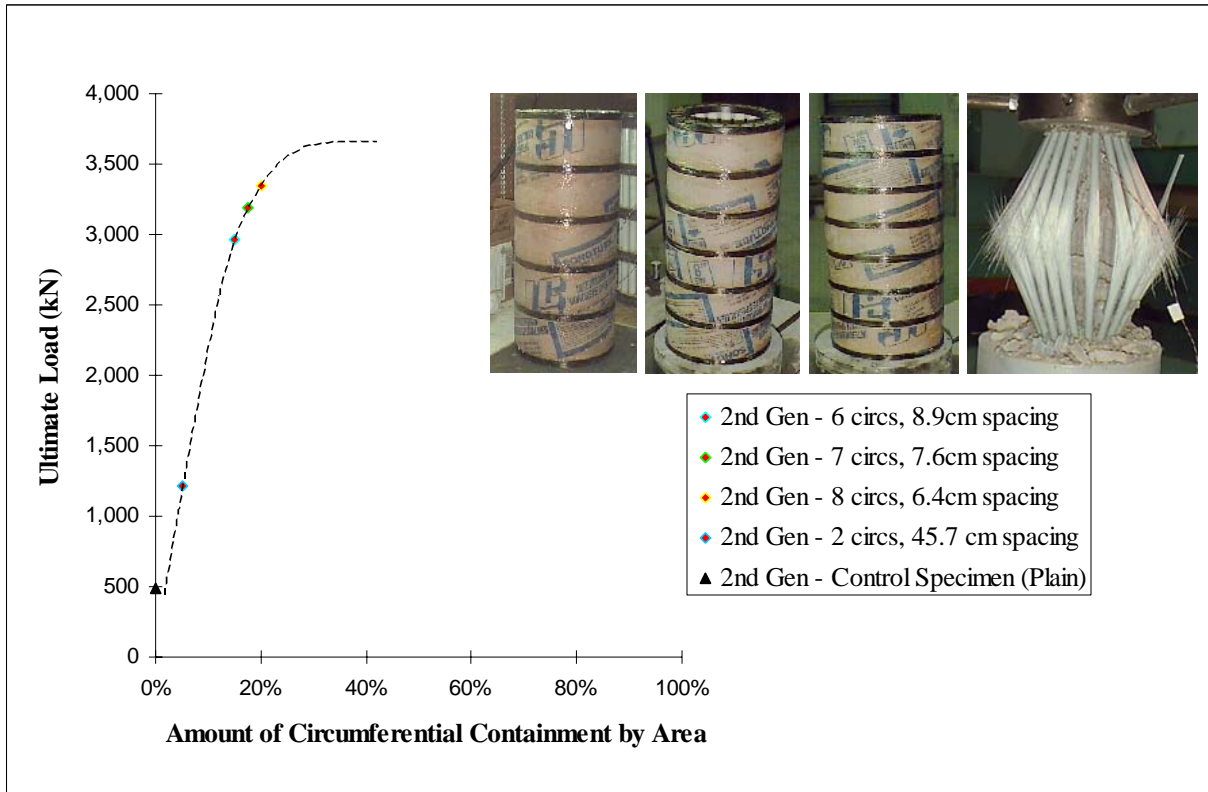


FIGURE 58 COMPARISON OF 2ND GENERATION COLUMNS IN AXIAL COMPRESSION BY AMOUNT OF CONTAINMENT

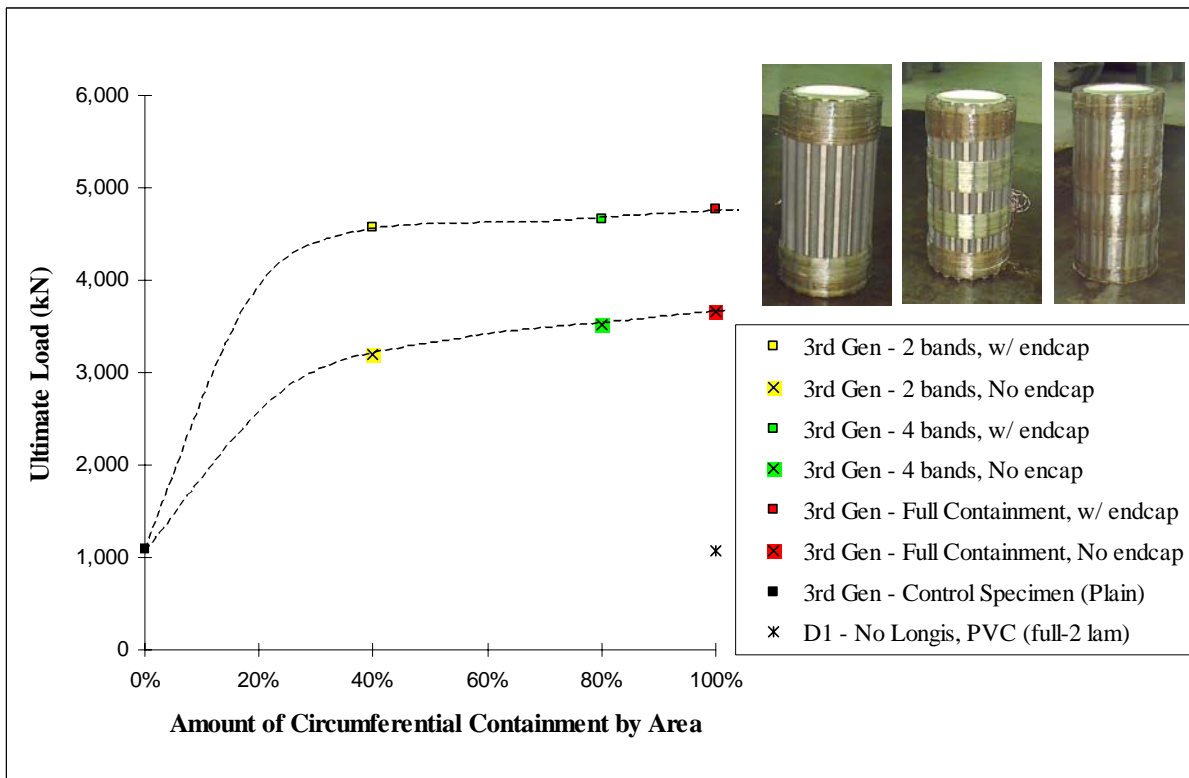


FIGURE 59 COMPARISON OF 3RD GENERATION COLUMNS IN AXIAL COMPRESSION BY AMOUNT OF CONTAINMENT

Because sections of the curves were unclear for 2nd and 3rd column generations, these plots were overlapped to compare these curves and complete the trend lines. Although different materials were used for containment in both of these grid structures, it was assumed that trend lines would be similar due to past similarities shown in stress-strain curves and load transfer behavior. These completed trend lines showed that approximately 90% of the ultimate load is reached by using only 30% circumferential containment of the surface area! (see Figure 60).

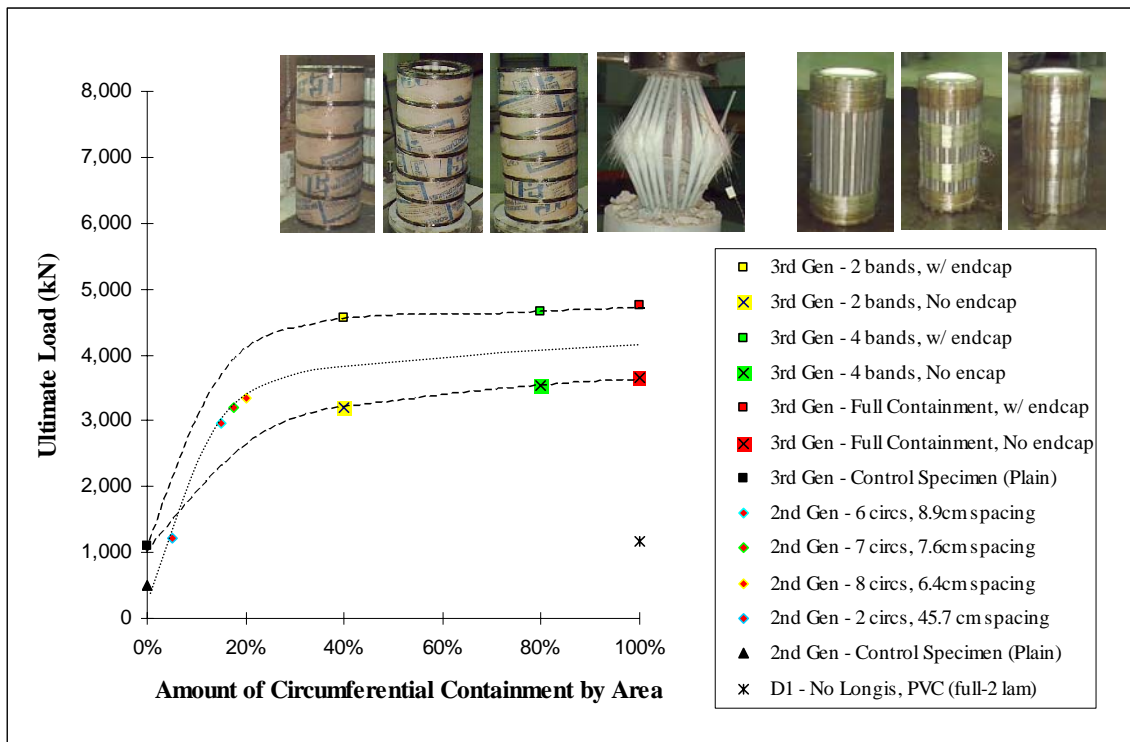


FIGURE 60 COMPARISON OF 2ND AND 3RD GENERATION COLUMNS BY AMOUNT OF CONTAINMENT

This figure suggests that the use of a strong, high quality containment material is effective in partial containment of concrete columns. Although ultimate load does not increase significantly after 30% circumferential containment is obtained, an important consideration is ductility. As shown in Table 7, ductility is a large benefit with the increase in containment; however, if ultimate load is more of a concern than toughness - partial containment is the answer. Costs of manufacturing, installing and strengthening concrete columns could be reduced considerably with the use of only a fraction of “full containment” while still maintaining a high ultimate load. The first generation columns were also added to this figure in order to show a similar trend line (see Figure 61).

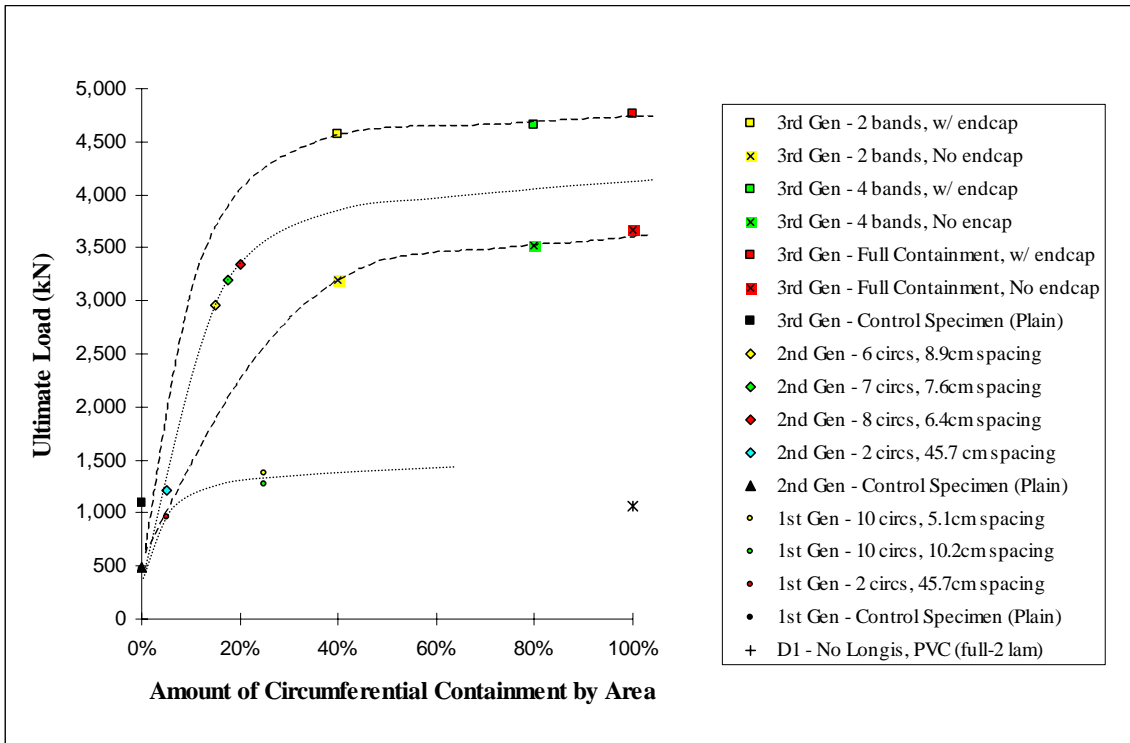


FIGURE 61 COMPARISON BETWEEN 1ST, 2ND, AND 3RD GENERATION COLUMNS BY AMOUNT OF CONTAINMENT

This comparison of ultimate load versus percentage of circumferential containment by area demonstrates how all three generations of these columns are linked together in their ability to resist shear due to axial compression.

CHAPTER 10

CONCLUSIONS AND RECOMMENDATIONS

10.1 CONCLUSIONS

The principle of partial containment works. More and stronger circumferential reinforcement clearly increases the axial compressive strength. The 2nd generation columns were three times stronger than the 1st generation columns, while the 3rd generation columns were stronger than both earlier generations with the ability to be applied to existing columns. This increase in strength was due to the high quality of the hoop windings, with a secondary contribution from the additional longis. The strength and spacing interval of the circumferential reinforcement couples with the stiffness and quantity of the longitudinal reinforcement to determine the ultimate compression strength of the advanced composite grid reinforced concrete columns. The ability of these grid reinforced columns to repeatedly release stress through failure of a top or bottom circle and then build up to an even higher load in a ductile nature makes them unique. The material characteristic of these advanced composite grid structures holds great promise for seismic applications when considering retrofit and rehabilitation of concrete columns.

These advanced composite grid structures are a “proof of concept” for controlling shear failure in concrete columns and increasing axial compressive strength of plain concrete columns by as much as 500%. Test results show that only 30% circumferential containment is needed to achieve approximately 90% the ultimate axial compressive load of a column with full containment. This suggests a significant cost reduction in materials and installation for partial containment compared to full containment which is currently used by industry today. The added benefits of light weight and corrosion resistance make these advanced composite grid structures a viable alternative to steel when considering the reinforcement and strengthening of concrete structures in the future.

10.2 FUTURE RESEARCH

Extensive research into the use of advanced composite grid reinforcement will be required before wide range acceptance can be achieved. The next step in this process will be to test these columns in flexure in order to determine ductility characteristics in bending. While



FIGURE 62 PHOTOGRAPH OF FAN-SHAPED LONGI FOR 4TH GENERATION COLUMNS

testing the first three generation of advanced composite grid structures, the need for optimized longitudinal reinforcement became important. A 4th generation column has been developed which uses fan-shaped longis with the proper dimensions to utilize all space around the outer diameter of an existing column (see Figure 62). These pultruded longis are placed on a filament wound mandrel and then the entire column is filament wound (see Figure 63).



FIGURE 63 PHOTOGRAPH OF FAN-SHAPED LONGIS ON MANDREL

Once the vinyl ester has cured the mandrel slips out of the center and the column is ready to be filled with high strength concrete (see Figure 64). This initial testing will give valuable data which can be used for design considerations when this technology is applied to existing concrete columns.



FIGURE 64 PHOTOGRAPHS OF 4TH GENERATION COLUMN FILLED WITH HIGH STRENGTH CONCRETE

In the near future these new pultruded longis will be applied to existing concrete columns in order to simulate a seismic retrofit. Flexure tests may also be performed on steel reinforced columns until failure and then this reinforcement can be used to simulate rehabilitation of a concrete column or pier after an earthquake strikes. While other rehabilitation methods require patching, pressurized grouting, and sand blasting of the existing column, this longitudinal reinforcement may be applied directly to the column and then wound with a fiber and resin combination similar to the rehabilitation method used by the Xxsys Robo-Wrapper.®

10.3 RECOMMENDATIONS

Although extensive research into the use of composite grid reinforcement will be required before wide range acceptance can be achieved, this field of structural engineering is growing rapidly. As appropriate design criteria and further research develops, a paradigm shift among practicing engineers will allow for the use of these materials in construction and industry. It is recommended that future work include:

1. Flexure tests on 4th generation columns using fan-shaped longis.
2. Comparison with steel reinforcement in axial compression and flexure.
3. Seismic retrofit of existing columns using 4th generation grid structure.
4. Rehabilitation of steel reinforced concrete column using 4th generation grid structure.
5. Optimization study performed on spacing and width of partial containment wraps.
6. Damping study performed on effect of composite reinforcement.
7. Fatigue testing.
8. Thorough cost analyses.
9. Explore scalability (full-scale testing).
10. In-place testing under actual conditions
11. Optimization of manufacturing process
12. Standardized design codes and practices

REFERENCES

- ACI Building Code and Commentary (1992), American Concrete Institute, pp. 318-389.
- American Concrete Institute (1995), ACI Building Code Requirements for Structural Concrete, pp. 319-395.
- Braestrup, M. (1997), Composite Approach. *Bridge Design and Engineering*, Nov. (9), pp. 23-24.
- Cercone, L. and Korff, J. (1997), Putting the Wraps on Quakes. *Civil Engineering*, ASCE, 67 (7), pp. 60,61.
- Chai, Y. H. and Priestley, M.J. (1991), Seismic Retrofit of Circular Bridge Columns for Enhanced Flexural Performance. *ACI Structural Journal*, 88 (5), pp. 572-584.
- Dunker, K.F. and Rabbat, B.G. (1995), Assessing Infrastructure Deficiencies: The Case of Highway Bridges. *Journal of Infrastructure Systems*, June, pp. 100-107.
- Dutta, P.K., et al. (1998), Composite Grids for Reinforcement in Concrete Structures: Construction Productivity Advancement Research (CPAR) Program. *US Army Corps of Engineers – USACERL Technical Report*, pp. 74-82.
- Gergely, I., Pantelides, C.P., Reaveley, L.D. and Nuismer, R.J. (1997), Strengthening of Cap Beam Joints of Concrete Bridge Piers with Carbon Fiber composite Wraps. *2nd National Seismic Conference on Bridges and Highways*, Sacramento, CA, July 8-11, pp. 599-508.
- Jones, A.J. (1996), Principles and Prevention of Corrosion. *2nd Edition*, Prentice Hall, Upper Saddle River, New Jersey 07458, pp. 387-390.
- MacGregor, J.G. (1997), Reinforced Concrete, Mechanics and Design. *3rd Edition*, Prentice Hall, Upper Saddle River, New Jersey 07458, pp. 224-228.
- Mander, J.B., Priestly, M.J.N., and Park, R. (1988a), Theoretical Stress-Strain Behavior of Confined Concrete. *Journal of Structural Engineering*, ASCE, 114 (8), pp. 1804-1826.
- Mander, J.B., Priestly, M.J.N., and Park, R. (1988b), Observed Stress-Strain Model of Confined Concrete. *Journal of Structural Engineering*, ASCE, 114 (8), pp. 1827-1849.
- Meier, U. and Kaiser, H. (1991), Strengthening of Structures with Carbon Fiber Reinforced Plastic Laminates. *Advanced Composites Materials in Civil Engineering Structures*, Las Vegas, Nevada, pp. 224-232.
- Meier, U. (1995), Strengthening of Structures Using Carbon Fiber/Epoxy Composites. *Sika[®] Carbo Dur - Structural Strengthening Systems*, pp. 341-351.

-
- Norris, T., Sاداتmanesh, H., and Ehsani, M.R. (1997), Shear and Flexural Strengthening of R/C Beams with Carbon Fiber Sheets. *Journal of Structural Engineering*, ASCE, 123 (7), pp. 903-911.
- Pantelides, C.P. and Halling, K.C. (1997), Carbon Fiber Composites for Rehabilitation of Bridge Bents and Columns. *2nd Symposium on Practical Solutions for Bridge Strengthening and Rehabilitation*. Kansas City, Missouri, pp. 283-292.
- Peters, S.T., Humphrey, W.D., Foral, R.F. (1991), Fibers and Resin Systems, "Filament Winding Composite Structure Fabrication." SAMPE®, Covina, California pp. 206-215.
- Priestley, M.J.N. and Park, R. (1987), Strength and Ductility of Concrete Bridge Columns Under Seismic Loading. *ACI Structural Journal*, 94 (2), pp. 206-215.
- Sاداتmanesh, H., Ehsani, M.R., and Limin, J. (1997), Repair of Earthquake-Damaged RC Columns with FRP Wraps. *ACI Structural Journal*, 94 (2), pp. 206-215.
- Sاداتmanesh, H., Ehsani, M.R., and Limin, J. (1996), Seismic Strengthening of Circular Bridge Pier Models with Fiber Composites. *ACI Structural Journal*, 93 (6), pp. 639-647.
- Sاداتmanesh, H., Ehsani, M.R., and Li, M.W. (1993), Behavior of Externally Confined Columns. *Fiber-Reinforced-Plastic Reinforcement for Concrete Structures*, Special Publication 138, American Concrete Institute, Detroit, 93, pp. 249-265.
- Seible, F., Priestly, M.J.N., Hegemier, G.A., and Innamorato, D. (1997), Seismic Retrofit of RC Columns with Continuous Carbon Fiber Jackets. *Journal of Composites for Construction*, ASCE, 1 (2), pp. 52-62.
- Seible, F., Hegemier, G.A., Priestly, M.J.N., Innamorato, D. and Ho, F. (1995), "Carbon Fiber Jacket Retrofit Test of Circular Flexural Columns with Lap Spliced Reinforcement," Structural Engineering, University of California, San Diego, La Jolla, California, Report No. ACTT-95/04, June 1995.
- Smart, C.W. and Jensen, D.W. (1997), Flexure of Concrete Beams Reinforced with Advanced Composite Orthogrids. *Journal of Aerospace Engineering*, 10 (1), pp. 7-16.